# CRYSTAL GROWTH, GUEST ORDERING AND FERROELASTIC PROPERTIES OF UREA INCLUSION COMPOUNDS

by

JEREMY RICHARD RUSH

B.A. William Jewell College, 1999

AN ABSTRACT OF A DISSERTATION

submitted in partial fulfillment of the requirements for the degree

DOCTOR OF PHILOSOPHY

Department of Chemistry
College of Arts and Sciences

KANSAS STATE UNIVERSITY
Manhattan, Kansas

2007

## Abstract

The ferroelastic urea inclusion compound (UIC) of 2,10-undecanedione/urea exhibits a striking pseudoelastic memory effect. Although pseudoelasticity is possible for UICs containing only 2,10-undecanedione, introduction of a structurally similar guest impurity (2-undecanone) gives rise to rubber-like behavior, a form of pseudoelasticity. This phenomenon depends on both the crystal strain and the concentration of monoketone: above 13-14% 2-undecanone, pseudoelastic behavior is observed reliably, even at strains as high as 2.4%. The dramatic change in ferroelastic behavior over a small range of impurity content indicates that this is a critical threshold phenomenon.

Because the impurity concentration has such a dramatic effect on domain switching, it was important to determine the sector-dependent patterns of incorporation of this relaxive impurity. Preliminary HPLC analyses of guest populations suggest that preferential incorporation of monoketone guests occurs between nonequivalent growth sectors, and that these patterns can be rationalized using a symmetry specific growth model. Birefringence mapping and HPLC studies of optically anomalous UICs containing mixtures of 2,9-decanedione and 2-decanone (which possess trigonal metric symmetry) suggest analogous patterns in guest incorporation and/or ordering that can also be rationalized. Although crystals of 2,9-decanedione/urea exhibit no ferroelastic strain at ambient temperature, they exhibit a proper ferroelastic phase transition near -170 ºC.

It is proposed that differential perfection of domains gives rise to pseudoelasticity in UICs, and that relaxive impurities play an important role in the energetics of this process. Because ultrafast video studies of domain reversion kinetics demonstrate no clear correlation of observed rates with impurity content, it is proposed that the relaxive impurities facilitate spontaneous domain reversion by annealing stressed defect sites that would otherwise lead to irreversible or plastic domain switching.

Following earlier work using synchrotron white beam X-ray topography, the driving force for domain reversion is thought to involve the presence of nanoscopic twins whose strain is epitaxially mismatched with neighboring daughter domains. The behavior of these nanoscopic twins was monitored with in-situ X-ray diffraction studies of stressed crystals, and this has led to a more thorough understanding of the role of these nanoscopic twins in the ferroelastic domain switching and rubber-like behavior in this class of materials.

# CRYSTAL GROWTH, GUEST ORDERING AND FERROELASTIC PROPERTIES OF UREA INCLUSION COMPOUNDS

by

JEREMY RICHARD RUSH

B.A. William Jewell College, 1999

A DISSERTATION

submitted in partial fulfillment of the requirements for the degree

DOCTOR OF PHILOSOPHY

Department of Chemistry
College of Arts and Sciences

KANSAS STATE UNIVERSITY
Manhattan, Kansas

2007

Approved by:

Major Professor
Mark D. Hollingsworth

## Abstract

The ferroelastic urea inclusion compound (UIC) of 2,10-undecanedione/urea exhibits a striking pseudoelastic memory effect. Although pseudoelasticity is possible for UICs containing only 2,10-undecanedione, introduction of a structurally similar guest impurity (2-undecanone) gives rise to rubber-like behavior, a form of pseudoelasticity. This phenomenon depends on both the crystal strain and the concentration of monoketone: above 13-14% 2-undecanone, pseudoelastic behavior is observed reliably, even at strains as high as 2.4%. The dramatic change in ferroelastic behavior over a small range of impurity content indicates that this is a critical threshold phenomenon.

Because the impurity concentration has such a dramatic effect on domain switching, it was important to determine the sector-dependent patterns of incorporation of this relaxive impurity. Preliminary HPLC analyses of guest populations suggest that preferential incorporation of monoketone guests occurs between nonequivalent growth sectors, and that these patterns can be rationalized using a symmetry specific growth model. Birefringence mapping and HPLC studies of optically anomalous UICs containing mixtures of 2,9-decanedione and 2-decanone (which possess trigonal metric symmetry) suggest analogous patterns in guest incorporation and/or ordering that can also be rationalized. Although crystals of 2,9-decanedione/urea exhibit no ferroelastic strain at ambient temperature, they exhibit a proper ferroelastic phase transition near -170 ºC.

It is proposed that differential perfection of domains gives rise to pseudoelasticity in UICs, and that relaxive impurities play an important role in the energetics of this process. Because ultrafast video studies of domain reversion kinetics demonstrate no clear correlation of observed rates with impurity content, it is proposed that the relaxive impurities facilitate spontaneous domain reversion by annealing stressed defect sites that would otherwise lead to irreversible or plastic domain switching.

Following earlier work using synchrotron white beam X-ray topography, the driving force for domain reversion is thought to involve the presence of nanoscopic twins whose strain is epitaxially mismatched with neighboring daughter domains. The behavior of these nanoscopic twins was monitored with in-situ X-ray diffraction studies of stressed crystals, and this has led to a more thorough understanding of the role of these nanoscopic twins in the ferroelastic domain switching and rubber-like behavior in this class of materials.

## Table of Contents

## List of Figures

**Chapter 5:**



**Chapter 7:**

**Acknowledgements**

This work is dedicated to my Family: Teresa, Jerry, Laura, Nick, Natalie, Jayla, Eddie, Trevor, Tara and Travis, who have supported me continually and without question; to Hellen, who reminds me that I'm not always in the right; to Magan, whose kindness makes life so much sweeter; to Mr. Robinson, who tried to instill the meaning of discipline; and, most importantly, to Elijah, who reminds me how wonderful it is to be curious.

# Chapter 1

## Introduction

The study of crystalline materials has contributed much to the understanding of solids and has lead to many advances in science and technology. From fiber optics to strong and lightweight metal alloys to ferroelectric memories, materials science[1] is ultimately responsible for many of today's technological innovations.

The study of solid materials is intimately linked with the discipline known as *crystal engineering*. Crystal engineering[2] has provided many insights into the nature of the solid state and how crystalline properties may be influenced or tailored to meet defined criteria. From the studies of Schmidt and Cohen,[3] Curtin and Paul,[4] Etter,[5] and McBride[6,7] on solid state interactions and reactivity, to the work of Ward,[8] Aakeröy[9] and Hosseini[10] on designing crystalline solids with specific, sometimes elaborate, forms of molecular recognition and properties, crystal engineering has grown from its foundations centered upon molecular recognition to encompass a wide variety of ideas, methods and discoveries.[11] Certainly, advances have been made in predicting and controlling factors such as crystal packing and bulk crystalline properties; however, there remain many misconceptions,[12] as well as promising areas of investigation, such as polymorphism[13] and the prediction of crystal morphology[14] and/or structure[15] in the landscape that encompasses crystal engineering and solid state chemistry. This thesis describes a contribution to this emerging discipline.

Of particular interest in this work is the class of materials known as the ferroics. A ferroic crystal (or polycrystal) possesses two or more *orientation states*, or regions of identical structure that differ in absolute orientation of their spontaneous strain, electric

polarization and/or magnetic moment.[16-18] Contiguous regions in a crystal that possess the same orientation state are known collectively as a *domain*. If a field or stress of sufficient strength is applied in the correct orientation relative to the orientation state, the domain may reorient, thereby populating another orientation state. The observable interconversion of orientation states, known as *domain switching,* is what defines ferroic behavior.[16-18] In general, there are three distinct ferroic properties: ferromagnetism, ferroelectricity, and ferroelasticity.[19] Ferromagnetic materials are probably the most popular of these. In a *ferromagnet*, unpaired electron spins are spontaneously aligned to produce a magnetic moment that may be reoriented by a magnetic field. For example, a pristine sample of iron may contain many disordered, ferromagnetic domains. Exposure to a strong magnetic field serves to align these into larger aggregates; more importantly, should the orientation of the magnetic field change, the orientation of the macroscopic domain can change with it. When this occurs, a second orientation state becomes populated. A magnetic material that can be switched from one magnetic orientation state to another is said to be *ferromagnetic*. (The prefix “ferro-” is derived from the Latin “ferrum,” meaning "iron".[20]) A mixed oxide of iron, lodestone, is thought to be the material in which ferromagnetism was first discovered.[21] (More appropriately, loadstone is not ferromagnetic, but is *ferrimagnetic*. In a ferrimagnetic material, magnetic domains of unequal strength are opposed so that, even though those domains are oriented antiferromagnetically, the net magnetic moment is nonzero.[22])

If a crystal produces an electric moment when subjected to an applied force, it is said to be *piezoelectric*.[23] This effect is observable in all noncentrosymmetric crystallographic point groups with the exception of 432. This phenomenon is to be

distinguished from the related *pyroelectricity*, in which a spontaneous electric moment changes as a function of crystal temperature.[23,24] *Ferroelectricity* is observed when the spontaneous electric moment exhibited by a crystal is capable of being switched between specific orientation states by an external electric field.[25]

The property of ferroelectricity is related to ferromagnetism in that at least two nominally degenerate orientation states (at null field) must be possible. However, instead of a magnetic moment, a ferroelectric material possesses an electric dipole moment that is reoriented by the electric field. In a similar manner, *ferroelastic* materials undergo domain switching between orientation states when subjected to an applied anisotropic force or *stress* (for example, compression along a particular direction). This property is observable because the crystal possesses a spontaneous *strain,* or distortion, from higher symmetry. For example, lead phosphate ($Pb_3(PO_4)_4$) is monoclinic (space group, C2/c) at ambient pressure and temperature.[26] In this crystal, the unit cell is distorted from trigonal metric symmetry by 2%. This distortion is achieved by lengthening one unit cell axis at the expense of shortening another. If a compressive force is applied to this crystal in a manner that counters the distortion, the ($Pb_3(PO_4)_4$) crystal will compensate for this force by rotating its unit cell orientation so that the distortion no longer opposes the force.

Ferroelectric and ferroelastic domain switching is illustrated in Figure 1.1. Here, a collection of unit cells in a domain exhibit either a spontaneous electric moment or a strain along the direction of the arrow. When an external perturbative field or stress is applied, this distortion becomes reoriented to accommodate the perturbation. For this process to occur, the orientation of the strain or electric moment must change, but the overall unit cell connectivity of the crystal remains invariant. (In the figure this

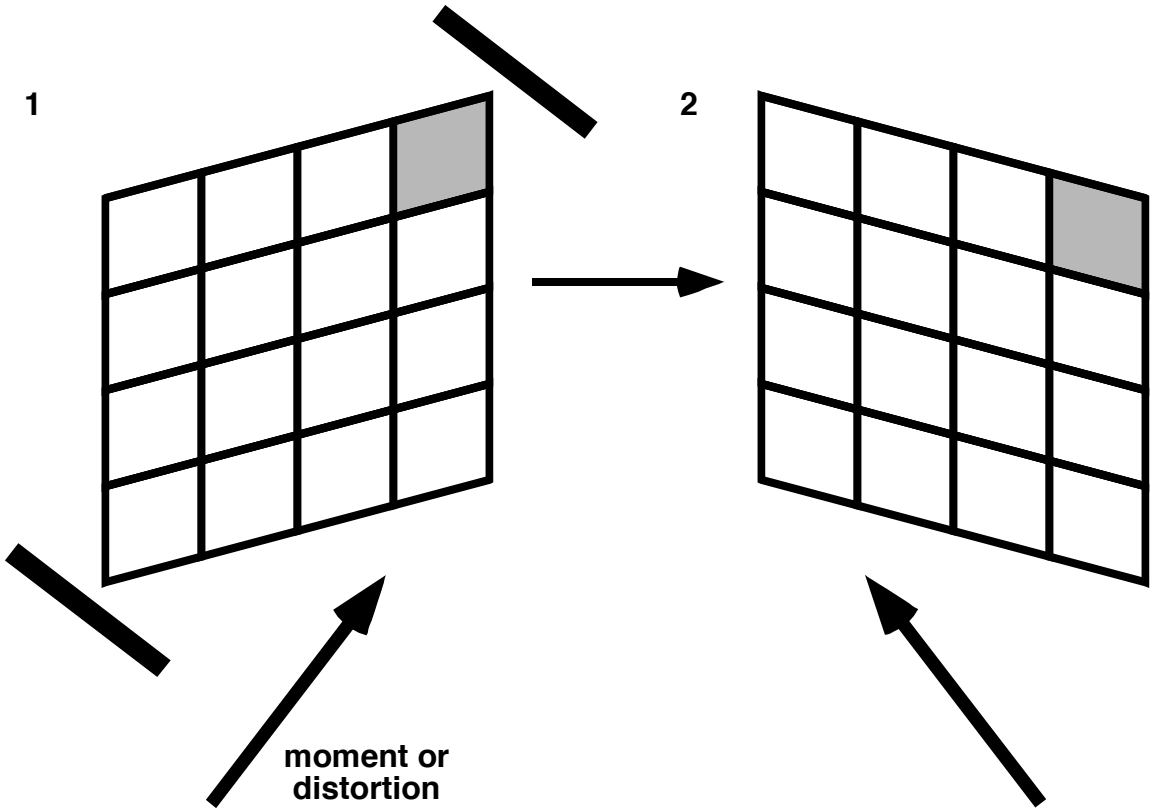


**Figure 1.1** Ferroelectric and ferroelastic switching involves the interconversion of unit cell orientations, or orientation states, when an anisotropic electric field or stress is applied. Here, the first orientation state possesses an electric moment or unit cell distortion along the direction of the arrow. When a field or stress is applied in a fashion that counters this moment or distortion, the atoms (or molecules) become reoriented in an accommodating fashion. The observable result is conversion of one orientation state (here, 1) into another (2). If the applied perturbation is an electric field, the material is said to be ferroelectric and the black bars represent electrically charged plates. If the perturbation is an applied stress or force, the material is said to be ferroelastic and the black bars represent a device for applying compressive force. In the absence of such perturbations, these orientation states are nominally degenerate.

invariance is illustrated by "labeling" one of the unit cells in grey.) In such an experiment the initial orientation state, or "mother," gives rise to a second orientation state, known as the "daughter." In the absence of the perturbative stress, the mother and daughter are isostructural and nominally degenerate,[16] so the daughter should persist if the field or stress is removed. Certainly, the application of an appropriate field or stress with respect to the daughter can cause it to reorient to the mother orientation.

The property depicted in Figure 1.1 describes the behavior of many ferroic materials.[18,27,28] However, an analogous, yet quite different phenomenon is exhibited by the *martensitic shape-memory alloys*. A *martensitic phase transition* is a diffusionless transition that involves lattice shearing[29,30] as one cools from the high-temperature, high symmetry (*austenite*) phase to the low-temperature, low symmetry (*martensite*) phase. Martensitic phase transitions are responsible for the hardening of steel and have been observed in many other metals and alloys. Although they are typically *disruptive* (that is, they involve discontinuous changes in symmetry such that one phase cannot be described using the "frame of reference" of the other[31]) a small subset of martensitic phase transitions is nondisruptive.[32] As discussed in Chapter 3, *ferroelastic phase transitions* are nondisruptive and are characterized by a change in point symmetry. It follows that a small fraction of nondisruptive martensitic phase transitions share properties of ferroelastic phase transitions.[32]

Some martensitic alloys, for instance, certain mixtures of tin and nickel,[33,34] exhibit the *shape memory effect*. When such an alloy has been deformed, mild heating to a threshold temperature results in a spontaneous return to its original shape. For certain shape memory materials, simple release of the perturbative stress yields the recovery of

the original shape; this effect is known as rubber-like behavior.[35,36] Shape memory phenomena will be discussed further in Section 1.2. The similarities between ferroelasticity and the shape memory effect means that an appreciation of shape memory alloys is relevant to the discussion of organic ferroelastics, which are the subject of this dissertation. At the same time, the study of organic ferroelastics can contribute much to the understanding of shape memory alloys.

The importance of ferroelectrics in materials science and technological applications demands a thorough understanding of their properties, which can lead to improvements and modifications of their properties. The motivation for the science reported herein lies in the observation that many ferroelectrics possess a spontaneous strain in addition to their spontaneous dipole moment. Should the strain and dipole moment reorient together during the domain switching event, the material is said to be a *ferroelastic ferroelectric*.[16] (Such materials are to be distinguished from piezoelectrics, which are a part of a broader class of materials that do not necessarily exhibit ferroic domain switching.) For instance, upon the application of an stress or electric field, crystals of gadolinium molybdate ($Gd_2(MoO_4)_3$) undergo domain switching that involves the concomitant reorientation of the spontaneous strain and dipole moment.[37] Because, for materials such as gadolinium molybdate, ferroelastic and ferroelectric properties are coupled, it appears plausible that, on a molecular level, these properties are intimately connected.[16] Thus, a thorough appreciation of ferroelectricity requires a deeper understanding of ferroelasticity.

The work described in this thesis involves the study of ferroelastic inclusion compounds of urea. The vast flexibility of synthetic organic chemistry provides the

experimentalist with an immense supply of molecules that can be constructed. Coupled with the reliable architecture of urea inclusion compounds, it is possible to tailor physical properties in a systematic fashion and to discern what factors control ferroelastic behavior. Upon gaining adequate insights into ferroelasticity, it may be possible to design ferroelectric materials with specific properties.

## 1.1 Urea and Urea Inclusion Compounds

Urea has a long history critical to the development of organic chemistry. In 1828 it was first synthesized in the condensation of ammonia and carbon dioxide by Wöhler.[38] This synthesis was a landmark achievement in the emerging discipline of organic chemistry because it demonstrated that chemicals found in living things can be produced synthetically; this contributed to the demise of the "vital force" theory that had long pervaded the physical sciences.[39,40]

Figure 1.2b-c present the crystal structure of urea. Though apparently a simple structure, the large degree of intermolecular cooperativity exhibited by a network of NH•••O hydrogen bonds makes modeling and the prediction of its crystalline properties difficult;[41-45] however, recent progress has been made in predicting crystal morphology[14] and attachment energies.[46] Urea is a useful *non-linear optic* (NLO) material: when exposed to light from a laser, crystals of urea emit a second signal with half the incident wavelength. [47]

Nearly 60 years ago Bengen and Schlenk[48] demonstrated that urea can form inclusion compounds when crystallized in the presence of a second component. In a *urea inclusion compound (*UIC), the urea *host* typically forms helical channels (Figure 1.2d-e)

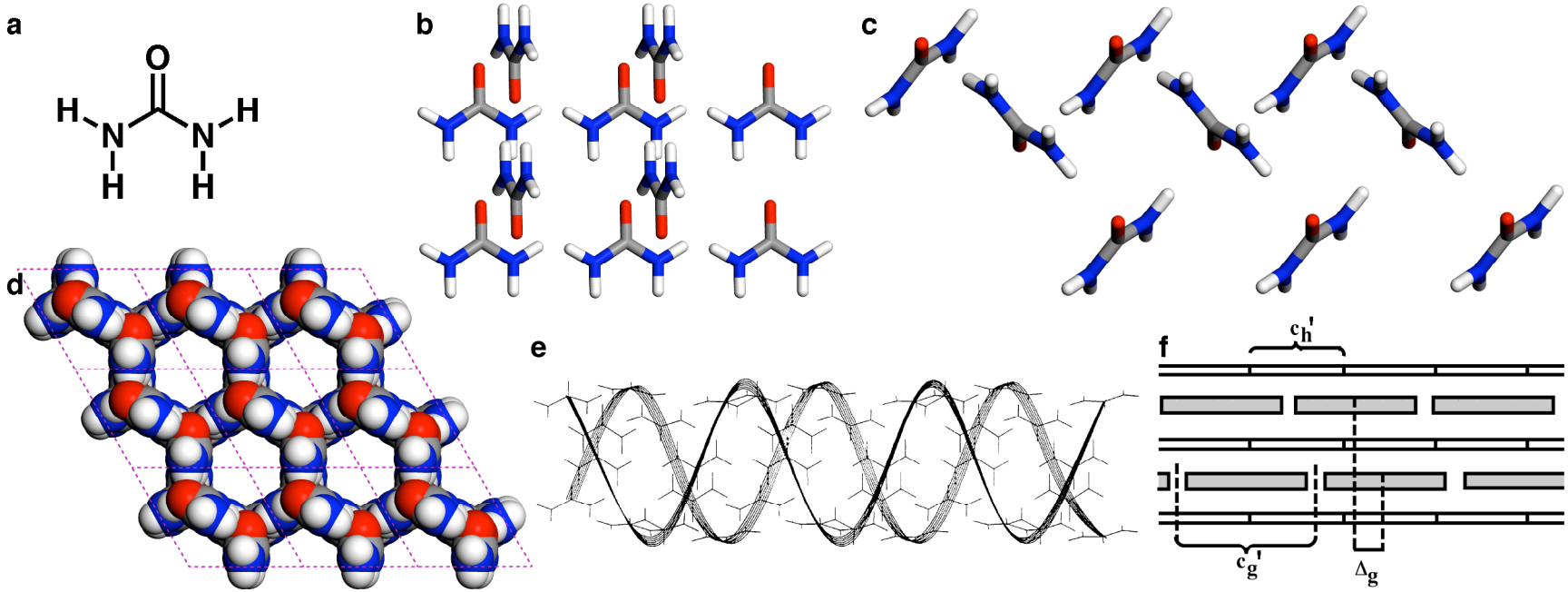


**Figure 1.2** Urea and urea inclusion compounds. (a) Urea forms a white crystalline solid at room temperature. In its crystal structure (**b**,**c**), pure urea exhibits a high degree of intermolecular connectivity through a series of NH•••O hydrogen bonds. Space group, $P\bar{4}2_1m$; $a = b = 5.565$ Å, $c = 4.684$ Å. (Drawn from 12 K neutron diffraction data of Swaminathan, *et. al.*, *Acta Crystallographica*, (1984) *B40*, 300. CSD refcode UREAXX12.) (**d**-**f**) In the presence of long-chain hydrocarbons, a urea inclusion compound (UIC) may form. In a UIC, the urea host forms a honeycomb-like network of hexagonal or pseudohexagonal channels inside which the hydrocarbon guest resides. (**d**) The host structure from hexadecane/urea, viewed along the [001] (channel) axis (guest atoms removed). Here, atoms are drawn with 100% van der Waals radii (C = 1.70, H = 1.20, N = 1.55, O = 1.52 Å). The inside diameter of the channels is about 5.5 to 5.8 Å; the channel centers are separated by about 8.2 Å. Space group $P6_122$; a = b = 8.227 Å, c = 11.017 Å. (Drawn from the room temperature X-ray data of Harris and Thomas, *Journal of the Chemical Society, Faraday Transactions*, (1990) *86*, 2985.). (**e**) By viewing the channel from its side, the pattern of hydrogen bonding between ureas is observable. As with tetragonal urea, this structure is held together by a series of NH•••O hydrogen bonds, but the intermolecular geometries of the two are different. Here, the backbones of each half of the urea double helix has been emphasized. (**f**) A schematic of a UIC, viewed from the same perspective as in **e**, with structural parameters of the host and guest emphasized. Each turn of the urea helix comprises 6 ureas and spans 11.0 Å. This repeat length is denoted by $c_h'$. The guest repeat length, $c_g'$, varies with guest. $\Delta_g$ describes the longitudinal offset between guests in neighboring channels. For the commensurate UICs central to the work described herein, $\Delta_g = 0$ Å. Images in **e** and **f** were adapted from Hollingsworth, *et al., Science (Washington, D.C.)*, (1996), 273, 1355.

around the long axis of the incorporated *guest*. The long, cylindrical channel best accommodates molecules of a similar shape; thus, the first UICs contained long-chain aliphatic fatty acids. As with pure urea (space group $P\bar{4}2_1m$),[49] the ureas in a UIC exhibit a large degree of intermolecular connectivity manifested in an extensive network of NH•••O hydrogen bonds.

As Figure 1.2d illustrates, the urea host molecules are oriented parallel to the channel wall; this provides a molecularly smooth channel interior with an inner diameter of 5.5 to 5.8 Å.[50] With van der Waals cross-sectional distances of somewhat less than 5 Å, linear hydrocarbons make suitable UIC guests.[51] The propensity for incorporation of aliphatic guests made urea inclusion compounds a favorite of the petroleum industry in the 1950s[52,53] because of their utility in separating mixtures of linear and branched hydrocarbons.

### 1.1.1 Registry Between Urea Host and Guest Dictates UIC Properties

Regardless of guest, for many urea inclusion compounds containing simple hydrocarbons (or those with minor substitutions), the ureas form helical channels that surround the linear guests. (In one type of alternative structure, discussed below, the channel is composed of stacked-loops of urea molecules.) The crystal structure of the urea host, taken from a study of hexadecane/urea,[54] is presented in Figure 1.2d. For this crystal, the host structure is hexagonal (space group $P6_122$ or $P6_522$) with $a$ = 8.227 Å and $c$ = 11.017 Å. Inspection of this structure reveals that the urea channel is composed of two intertwined helices that run in opposite directions along [001]. (For this and most other UIC structures discussed in this thesis, the $c$-axis and the channel axis are

collinear.) In the UIC, the 11.0 Å host repeat length corresponds to a complete turn of each urea helix, which is composed of six ureas. Thus, the channel "pitch" is approximately 1.84 Å per host molecule. These urea host metrics are preserved in most UICs exhibiting the helical channel structure.

The UICs formed by most hydrocarbons possess in common one additional feature: they are nonstoichiometric for host and guest. For the many guests known to form UICs, each possesses a preferred length when in its fully extended conformation. Since the hydrocarbon chain of the guest runs parallel to the host channel, the repeat lengths of host and guest (or integral multiples of these) must coincide in order for a rational host-guest stoichiometry to be achieved. This requirement is expressed by the relation:

$$mc_g = nc_h \tag{1}$$

where $c_g$ is the average length (along the channel axis) per guest and $c_h$ is the average channel repeat length (11.0 Å). *Commensurate* UICs have reasonably small values of *m* and *n* that satisfy the above equality; *incommensurate* UICs do not. In commensurate crystals, the guest molecular length and the 11.0 Å host channel repeat length are expressed as $c_g'$ and $c_h'$ respectively.[51] For example, *n*-pentadecane ($C_{15}H_{32}$) spans 21.11 Å in the UIC,[55] which is approximately 0.9 Å shorter than the 22.0 Å length of two helical repeats. For $12c_g' = 23c_h'$ (253 Å length) there exists a possible commensurate relationship; however, this relationship has not been observed experimentally, and *n*-pentadecane/urea is thought to be incommensurate.[55] Currently, all alkane/UICs that have been investigated with high resolution methods are thought to be incommensurate at room temperature.[55,56] (Because much of the early work[57,58] employed photographic X-

ray methods, conclusions of incommensurate behavior made on the basis of such measurements should be questioned. Further studies, using high resolution X-ray area detectors, may provide examples of commensurate alkane UICs.[59]) Nevertheless, some UICs of alkanes exhibit a commensurate structure at reduced temperatures.[55] One example is hexadecane/urea, which is commensurate below 129 K, with $8c_g' = 16c_h'$ (176 Å repeat length).

Many UICs are formed by guests that possess some sort of directing element that forms a specific interaction with the host. Structural "directing" elements include hydrogen bonding and bulky substituents, which can provide greater strength and specificity of host-guest interactions than simple van der Waals contacts exhibited by unbranched alkanes.[51] Examples include long-chain diacyl peroxides,[60] symmetric anhydrides[61] and α,ω-dihaloalkanes.[62] In the last case, the guest contains no hydrogen bond acceptor, but the substitution of a methyl group with a halogen is thought to alter the interaction between host and guest. Although many of these crystals are thought to be incommensurate,[51,63] interaction between host and guest leads to interchannel guest cooperativity that is manifested as consistent interchannel guest offsets ($\Delta_g$, Figure 1.2f) within in each series. For instance, peroxide guests of varying chain lengths are translated 4.6 Å along [001] ($\Delta_g$ = 4.6 Å) from their neighbors in adjacent channels. This is in contrast with the dihaloalkanes,[62] for which $\Delta_g = c_g/3$, and with the anhydrides[61] and the alkanes,[64,65] for which guests are arranged side by side in the channels ($\Delta_g$ = 0 Å). (For one anhydride, heptanoic anhydride, $\Delta_g$ = 2.3 Å at room temperature and 1.5 Å and 0 Å in lower temperature phases.[61,66] Although it has been speculated that the unique behavior of heptanoic anhydride/urea may result from a commensurate structure, this has

not been demonstrated.[66]) The observation of series of incommensurate UICs with constant values of $\Delta_g$ suggests that some sort of specific ordering interactions are operative in these crystals. For UICs formed from bis(methyl ketone) guests, which are discussed more fully in Section 1.1.2 and which are the subject of much of this thesis, $\Delta_g$ = 0 Å.[67]

An alternative topology, in which hydrogen bonded hosts form "stacked-loop" hexamers, is observed for guests of structure $X(CH_2)_6Y$, where X and Y = Br, Cl, CN, NC and mixtures thereof.[51,68,69] For these, the commensurate relationship $c_g' = c_h'$ is observed, and the space group is often $P2_1/n$. Crystals such as 1-chloro-6-cyanohexane/urea exhibit interesting properties, including a thermal phase transition in which guests are translated by 5.5 Å along the channel.[68] For UICs of 1.6-dibromohexane, 1,6-dichlorohexane, and 1-bromo-6-chlorohexane, two guest conformers are observed. Using $^2H$ NMR and X-ray data from 1,6-dibromohexane/urea,[69,70] two *gauche* conformers were observed at the chain termini. At low temperatures, one conformer predominates so that the host channel becomes distorted along [100]; as the temperature is raised, an increase in population of a second gauche conformer evens out this distortion, and the crystals approach hexagonal metric symmetry.[69] Although stacked-loop UICs provide an important structural counterpart to helical UICs, they will be discussed only in the context of memory effects in ferroelastic UICs (Sections 4.2 and 4.3).

The work described herein deals primarily with helical channel UICs based on a series of bis(methyl ketone) guests and their analogues. Although most of these are commensurate, interactions between host and guest exhibited by each leads to important

differences in the symmetry relationships that describe these crystals. These differences are manifested in a variety of properties that include the characteristics of guest incorporation, optical and crystallographic features, and ferroelastic properties.

### 1.1.2 UICs of Bis(methyl ketone) Guests

In 1995 Brown and Hollingsworth reported the crystal structure of 2,10-undecanedione/urea (Figure 1.3).[71] Because of the hydrogen bonds between guest carbonyls and urea N-H groups, this crystal differs from the prototypical UIC structure presented in Figure 1.2. For 2,10-undecanedione/urea the degree of host-guest connectivity provided by this interaction is crucial to its crystalline properties. Indeed, no commensurate repeat is expected for an alkane guest consisting of eleven carbons (for undecane, the predicted $c_g$ = 16.3 Å).[58] However, 2,10-undecanedione/urea exhibits a commensurate relationship of $2c_g' = 3c_h'$ and has a repeat length of 33.0 Å along the channel, or 16.5 Å per guest.

The crystal structure of 2,10-undecanedione/urea is illustrated in Figure 1.3c. Here, the guests are arranged in an antiferroelectric manner with their carbonyls directed along [100]. Along the {100} channel walls, every third urea (colored in red) rotates by 32.59° about its C=O bond so that it may form $NH_{syn}$•••O hydrogen bonds to guest carbonyls on either side of the channel wall.[72] (This angle was determined by measuring the angle between the (100) channel wall and the vector connecting the two nitrogens on the rotated urea.) Each guest carbonyl forms a hydrogen bond with a host urea so that each end of the guest molecule is "tethered" to the host, resulting in a large degree of host-guest connectivity. Since the natural length of an alkane containing eleven carbons is shorter than the 16.5 Å guest length required by the commensurate relationship, the

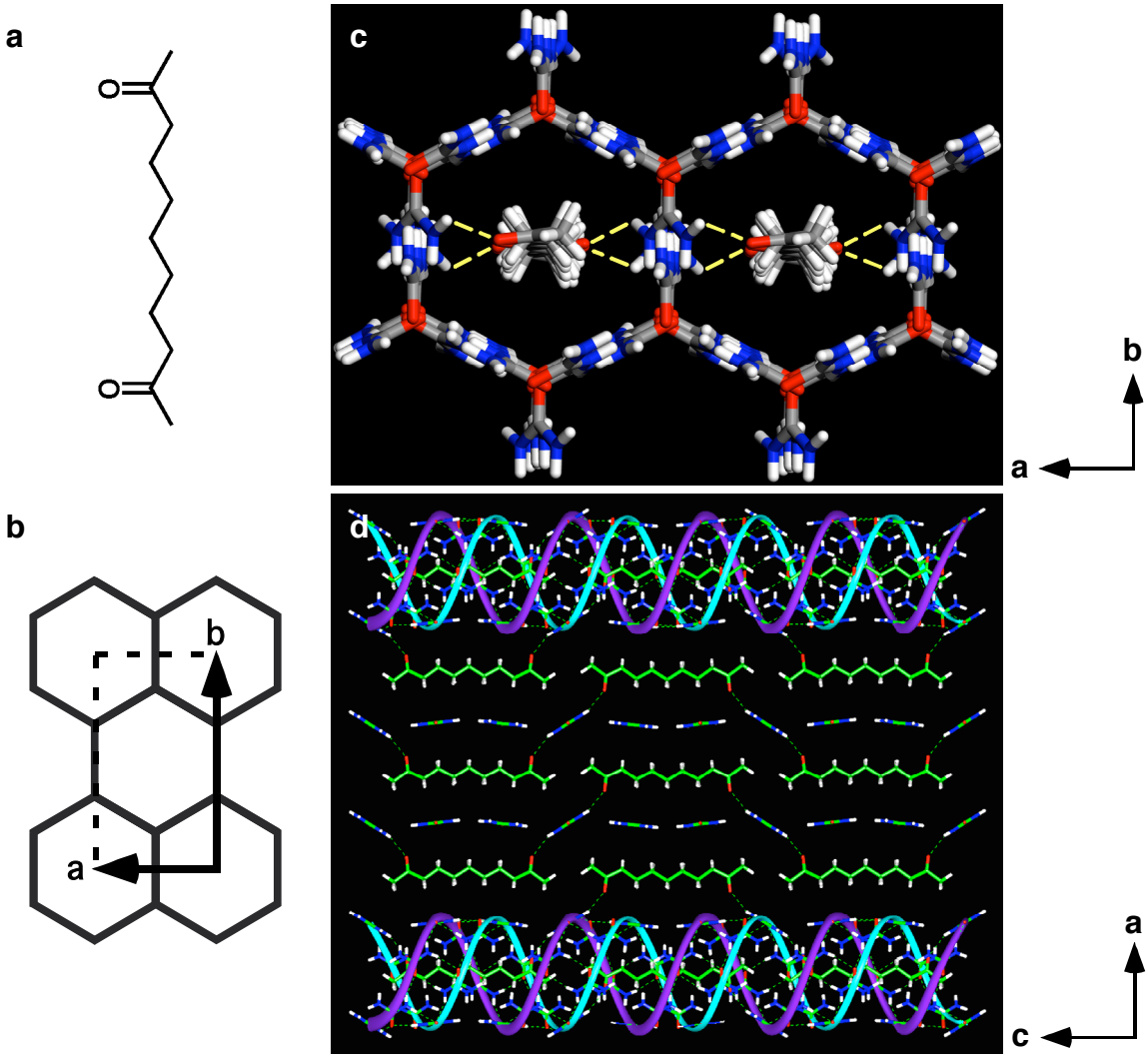


**Figure 1.3** **(a)** 2,10-undecanedione. The urea inclusion compound of of this guest is commensurate, with $2c_g' = 3c_h'$. **(b)** The crystal structure incorporates two urea channels per orthorhombic unit cell (dotted lines). **(c)** The crystal structure of 2,10-undecanedione/urea determined from data collected at room temperature. Here, two channels are viewed along [001] (the channel axis) from the same vantage shown in **b**. Within the channels, guests are oriented with their $CH_2$ and carbonyl groups toward the horizontal {100} channel walls and form hydrogen bonds with ureas there (yellow dotted lines). Between channels, guests at the same longitudinal position are oriented in the same direction; in this image, the carbonyl groups for the frontmost guests are all oriented along [100]. **(d)** Side-view of the crystal structure, along [010]. Within each channel, adjacent guests are related by a $2_1$ axis. This results in the antiferroelectric ordering of guests observed in this image. Each donor urea donates hydrogen bonds to guests in two adjacent channels; this makes possible the hydrogen-bonded network of host-guest-host-guest, etc., that ensures a large degree of interchannel interaction. Image **c** was drawn from the data of Brown and Hollingsworth, *Nature (London)*, **376**, 323 (1995). Image **d** was adapted from the above reference. Space group $C222_1$; $a$ = 8.345 Å, $b$ = 13.939 Å, $c$ = 32.982 Å (at 293 K). Host-guest hydrogen bond geometry: N•••O, 3.019 Å; (urea)CN•••O, 149.5°; (ketone)CO•••N, 142.3°.

terminal methyl groups of neighboring guests are beyond van der Waals contact. The energy cost of this reduced packing efficiency is probably offset by the host-guest hydrogen bonding. Further consequences of such connectivity will be discussed more thoroughly below and in later chapters.

The crystal structure of 2,10-undecanedione/urea reveals additional interesting features. Because the hosts are located on the channel walls, the ketone guest must direct its carbonyl (and much of the methylene chain) towards those walls in order to form hydrogen bonds with the ureas there. This observation coincides with the structural view of Chatani and coworkers,[73,74] in which the methylene chains of linear hydrocarbons are oriented towards the channel faces at high temperatures, and toward the vertices at low temperatures. (However, this observation contrasts an early structural model, in which alkyl chains are directed toward the more spacious vertices.[75] Additional disagreement[76,77] involves the number of possible orientations populated by guest molecules at low temperatures; owing to inconsistencies in the appearance of published diffraction patterns, this matter has yet to be resolved.[51]) With 2,10-undecanedione/urea, the orientation of guest toward the channel face gives rise to a slight distortion of the nominally hexagonal urea channel: the channel is strained along [100] by about 3.7% at room temperature. The symmetry for this crystal is therefore not hexagonal, but orthorhombic, with space group $C222_1$.

The ferroelastic distortion exhibited by 2,10-undecanedione/urea is a necessary condition for ferroelasticity. As shown in Figure 1.4 (adapted from the work of Brown and Hollingsworth[71]), this strain can be reoriented when a stress of suitable force and orientation is applied. For this UIC, the direction in the *ab* plane (i.e., perpendicular to

the urea channel) along which the refractive index is the largest is said to be the *slow axis* in that projection. For 2,10-undecanedione, this axis is parallel to [100] and, therefore, the strain. (The fast axis in the *ab* plane runs parallel to [010].) When the crystal is oriented as shown in Figure 1.4a, the slow axis is coincident with one of the microscope polarizers (one of which is oriented along the vertical and the other along the horizontal) so that the crystal appears dark, or *extinguished*. (For all of the experiments discussed in this thesis, the term "slow axis" will be used to describe the direction of largest refractive index in the *ab* plane. However, for crystals of 2-decanone/urea, the largest component of the refractive index tensor (*indicatrix*) runs parallel to the channel axis;[78] it is quite likely that the same is true for 2,10-undecanedione/urea.) When stress is applied to appropriate {110} faces of this crystal, ferroelastic switching occurs so that portions of this crystal are no longer in the extinguishing position. These reoriented "daughter" domains have their slow axes oriented approximately 60° from the mother domain and perpendicular to the applied stress. Because the distortion in the *ab* plane runs parallel to the slow axis, it follows that this crystal has accommodated the compressive stress by undergoing ferroelastic reorientation. This phenomenon will be discussed below and in Chapters 4 and 5.

This remarkable property exhibited by crystals of 2,10-undecanedione/urea has inspired a program of research with the primary focus of understanding and controlling the factors that influence ferroelasticity in molecular crystals. To learn about these properties, it has been necessary to study a large variety of urea inclusion compounds containing various guests and mixtures of guests. For example, a closely related series of UICs is based on the guest 2,9-decanedione. This guest is structurally very similar to

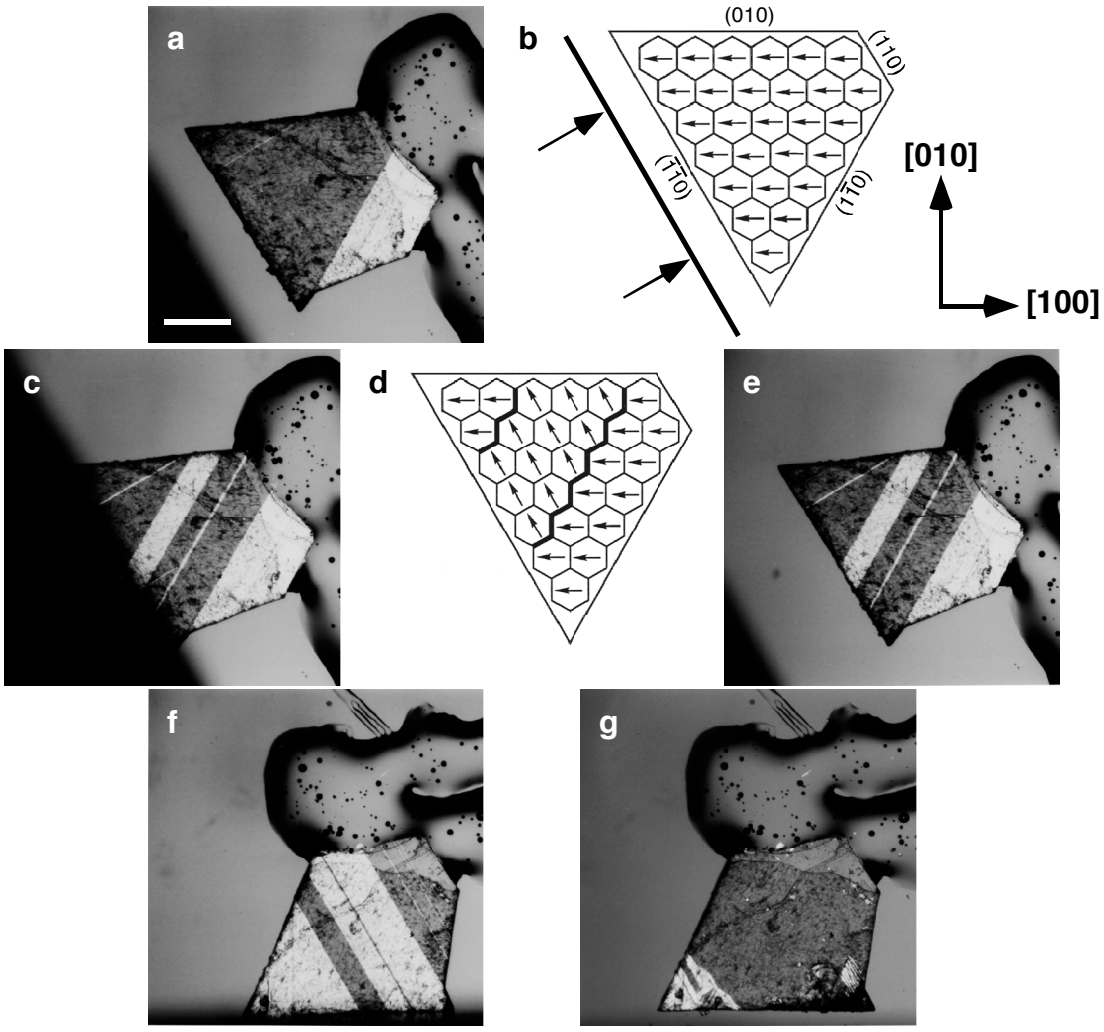


**Figure 1.4** Ferroelastic domain switching in a crystal of 2,10-undecanedione/urea. Photographs **a, c,** and **e-g** were taken between crossed polars and with a λ plate. Scale bar = 0.50 mm. **(a)** The crystal prior to the application of stress. Here, it has been fastened with epoxy resin (at right). The dark portion of the crystal is in the extingusihing position: the largest refractive index in the ab plane is aligned horizontally so no little or no light passes. For this parent (*mother*) domain, one layer of the guest carbonyls (which are parallel to the strain axis and the slow axis) are represented by the arrows in **b**. In this schematic the [001] and [010] axes are labeled, along with relevant growth faces. For this orientation of strain (along [100]), ferroelastic domain switching is induced by compressing the crystal between {110} faces. (The stress anvil is depicted in **b**.) In **c**, the stress has caused some channels to reorient – these regions are known as *daughter domains*. Because the slow axis for these channels is no longer horizontal, these regions of the crystal are no longer extinguished. **(d)** A schematic diagram of the mother and daughter in this crystal. Here, the strain in the daughter has rotated approximately 60° clockwise and is perpendicular to the axis of compression. The domain boundary between the two domains is in bold. **(e)** Upon removal of the stress, the daughter is permanent, or *plastic*. **(f)** The daughter extinguishes when the crystal is rotated 60° counterclockwise; this confirms the orientational assignment provided in **d** and that this is a single-crystal to single-crystal transformation. **(g)** Following repeated applications of stress a large majority of the crystal has been converted to daughter, which is exinguished in this orientation (as in **f**). Some damage has occurred in the lower right-hand corner of the crystal, so this region does not appear extinguished. Figure adapted from Brown and Hollingsworth, *Nature (London)*, **376**, 323, (1995).

2,10-undecanedione but is one methylene shorter. This apparently minor difference between guests contributes to appreciable differences in the properties their UICs. Crystals containing 2,9-decanedione/urea are commensurate with $3c_g' = 4c_h'$ and a channel repeat length of 44.16 Å.[79] As observed in 2,10-undecanedione/urea, 2,9-decanedione guest carbonyls are directed toward the channel walls so that hydrogen bonds can be formed (Figure 1.5). However, for this crystal the guest is too long: gas phase molecular mechanics calculations (conducted at the AM1 level of theory[80]) for the fully extended conformation of 2,9-decanedione indicate a C1-C10 distance of 11.32 Å, which is 0.34 Å longer than the distance observed[79] in the room temperature crystal structure of 2,9-decanedione/urea (10.982 Å). In the UIC, this guest therefore coils about its long axis and shortens so that it can form hydrogen bonds with the host and generate a commensurate structure. Within each commensurate repeat, three guests are related by a threefold screw axis along the [001] channel, and the structure is metrically trigonal (space group $P3_112$ or $P3_212$).

Because crystals of 2,9-decanedione/urea are trigonal and therefore lack spontaneous distortion, they are not ferroelastic. However, the study of this system has provided many insights into the general properties of urea inclusion compounds, including the characteristics of crystal growth and the consequences of structural ordering between host and guest. (Both are discussed in Chapter 2.) One important feature of 2,9-decanedione/urea (and the homologous 2,12-tridecanedione/urea[81]) is the presence of chiral twinning. In a microscope between crossed polars, crystals of 2,9-decanedione/urea appear uniaxial (Figure 1.6). However, when the polarizers are adjusted so they are not quite crossed (and the λ-plate is removed), optical rotation due to

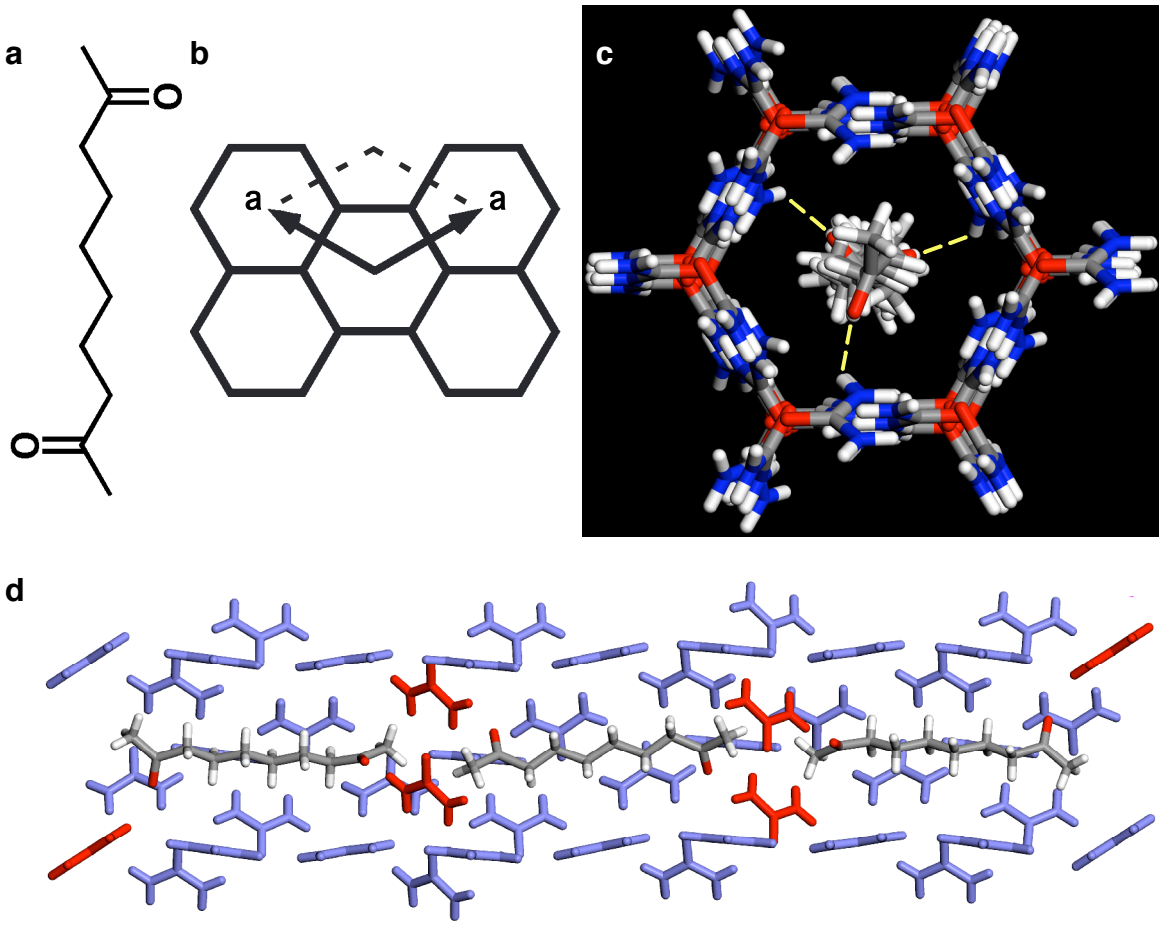


**Figure 1.5** 2,9-decanedione/urea. **(a)** The chemical structure of the guest. The urea inclusion compound of this guest is commensurate, with $3c_g' = 4c_h'$ and space group $P3_112$. **(b)** A view down the channel axis (along [001]); here, the trigonal unit cell is denoted by the dotted lines. **(c)** The crystal structure of 2,9-decanedione/urea, again viewed down the [001] (channel) axis. Because this guest is longer (by an estimated 0.34 Å) than optimal for a commensurate repeat of $3c_g' = 4c_h'$, the alkyl chain must coil up and shorten. This coiling makes the intramolecular O=C---C=O torsion angle approximately 106° instead of 180°, as anticipated for an extended conformation. This unfavorable guest torsion is offset by the formation of hydrogen bonds with the host. The carbonyls located at each end of the guest are directed toward the channel walls, where they form hydrogen bonds with ureas. The diagonal guest-host-guest hydrogen bonds ensures a large degree of host-guest interaction. **(d)** A side-view of the channel, along [110]. (For this perspective, the view in **c** was rotated 90° CW from the top.) The channel wall in front has been removed, and ureas forming hydrogen bonds with guests are colored red. The 120° rotational relationship of the guests is apparent in this image. Each urea forms hydrogen bonds with guests in two channels, as illustrated near the center. Drawn from data of Hollingsworth, et al., *Science (Washington, D.C.), (1996)*, *273*, 1355. Space group $P3_112$; $a = b = 8.229$ Å, $c = 44.16$ Å (at 294 K). Host-guest hydrogen bond geometry: N•••O, 2.964 Å; (urea)CN•••O, 141.4°; (ketone)CO•••N, 143.9°.

the helical host structure becomes visible. The acentric nature of the urea helix allows either left- or right-handed helices to form. Because they are simply enantiomorphs, the presence of helices of both senses of handedness within the same crystal is a form of crystal twinning. As the figure illustrates, individual growth sectors of 2,9-decanedione/urea can include chiral twins. Although an empirical correspondence linking right-handed ($3_1$) urea helices to levorotatory optical behavior has been derived,[82,83] a rigorous correlation between handedness and optical rotation has not been established. Nevertheless, the presence of chiral twins can have a profound impact on guest incorporation and ferroelastic domain switching. These phenomena will be discussed in Chapters 2 and 4.

The crystal structures of 2,9-decanedione/urea and 2,10-undecandione/urea demonstrate an important theme: the interaction between host and guest plays a decisive role in the crystal growth, stability, and overall properties of the UIC. Incorporation of 2,9-decanedione or 2,10-undecandione changes the crystal symmetry from the nominally hexagonal symmetry observed[54] in alkane UICs. In addition, there is a marked change in habit between UICs of these guests and those containing alkanes. Thus, interactions between host and guest can dictate the structural properties of the UIC. As demonstrated in later chapters, the reliability of the host framework and the adjustability of the guests it incorporates provide the experimentalist a handle with which the physical properties of urea inclusion compounds may be tailored.

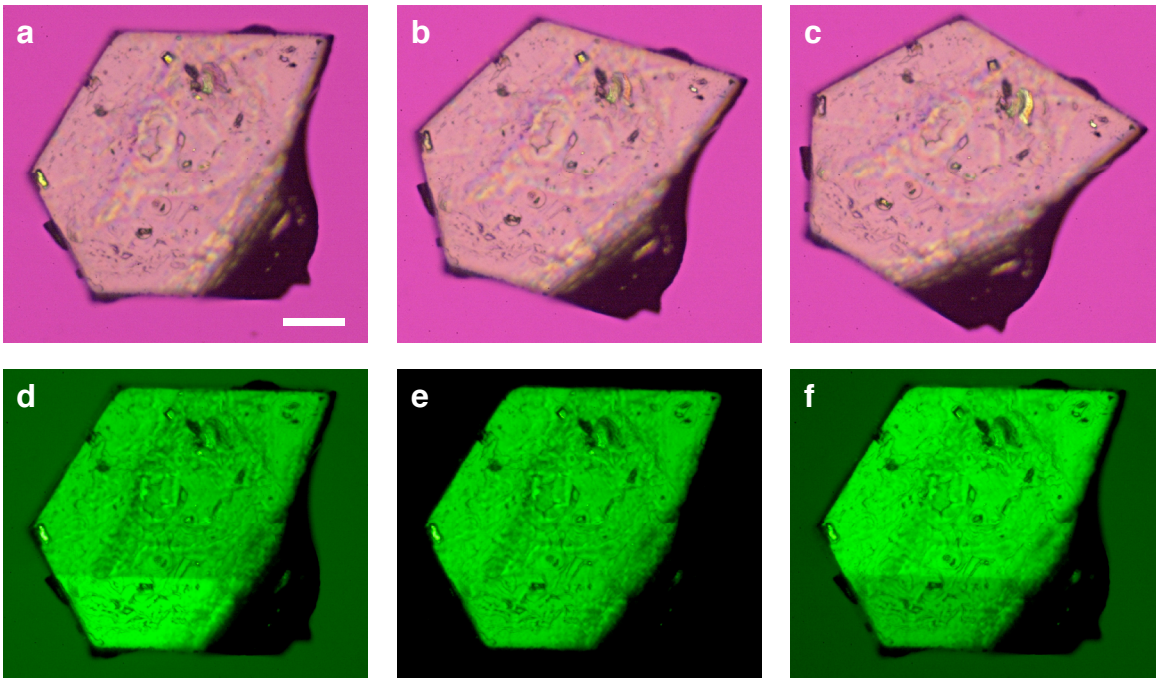


**Figure 1.6** Owing to their trigonal crystallographic symmetry (Figure 1.5), crystals of 2,9-decanedione/urea are optically uniaxial. Because, for a uniaxial crystal, the index of refraction in the plane perpendicular to the optic axis is the same regardless of the direction of polarization, the crystal appears extinguished regardless of orientation. For 2,9-decanedione/urea, the optic axis is the channel axis (or [001]), which runs perpendicular to the plate-face of the crystal. In **a-c** a crystal of 2,9-decanedione/urea is viewed along its optic axis. Because refractive index of the crystal is constant in all directions, its colors or brightness do not appear to change as the crystal is rotated. In photomicrographs **a**, **b** and **c**, optical rotation from the chiral channel permits the passage of some light between the crossed polars so that the crystal is not quite extinguished (it appears brighter than the magenta background). This phenomenon is discussed below. Scale bar = 0.20 mm (Nikon 5x). **(d-f)** Between uncrossed polarizers, the intensity of light passing through a chiral crystal will vary according to the magnitude (and direction) of rotation. (To reduce the effects of optical rotatory dispersion – wavelength-dependent rotation of white incident light – a green interference filter (GIF) was used instead of a λ plate for these images.) In practice the polars are "uncrossed" by rotating the analyzer while leaving the polarizer fixed. When the analyzer is rotated clockwise from the vantage of the observer (to "negative" numerical values), dextrorotatory (+) regions appear dark and levorotatory (–) regions appear bright. When the analyzer is rotated counterclockwise (to "positive" numerical values), the opposite effects occur. By comparing this behavior to the appearance of the crystal between crossed polars, the optical rotation (and hence, the chirality of the crystal or chiral twins within the crystal) may be discerned. **(d)** Crystal oriented as in **a**. Analyzer at –10°. Here, dextrorotatory regions appear darker than in **e**. **(e)** Crossed polars. No contrast between dextro- and levorotatory regions should be observable. **(f)** Analyzer at +10°. In this image, levorotatory regions appear darker than in **e**. The behavior of this crystal in **d**-**f** indicate that it is composed of channels of both handedness; the top portion is dextrorotatory and the bottom portion is levorotatory. The cause of increased brightness in the upper left-hand portion of this crystal in photos such as **d-f** is unknown. Between crossed polars and with a λ plate this effect is not observed. Dauphine twinning, observed in 2,12-tridecanedione/urea (Hollingsworth, et al., *Angewandte Chemie, Int. Ed.*, (2002), *41*, 965), involves a 180° rotation along the trigonal axis (Cahn, *Advances in Physics,* (1954), *3*, 363). However, this sort of twinning is not observable using the optical methods described.

### 1.1.3 Helical Wheel Diagrams: A Tool for Predicting Guest Geometry

Since host-guest hydrogen bonding is a primary directing element in UICs containing guests such as 2,10-undecanedione or 2,9-decanedione, it would appear that factors influencing the capacity for host-guest hydrogen bonding (for instance, the topology of the urea channel and the molecular length of the guest) will also affect the structural properties imparted by host-guest connectivity. It is therefore important to consider the patterns exhibited by the hydrogen bonding networks. For instance, in Figures 1.3 and 1.5 it is clear that hydrogen bonding occurs with particular ureas along certain channel walls. In general, the channel structure of all bis(methyl ketone) UICs is similar: the 11.0 Å repeat of the host helix and the relative positions of ureas along the channel are relatively invariant. It appears, then, that the hydrogen bond topology of these systems can be described by considering how each guest can form hydrogen bonds to ureas arranged in a prototypical, hexagonal channel.

Helical wheel diagrams (Figure 1.7) have proven invaluable as tools for predicting and rationalizing host-guest hydrogen bonding patterns for the UICs of bis(methyl ketones).[67,81] For these materials, ureas along the channel are numbered in both helices (1, 2, 3, etc., for one helix and 1', 2', 3', etc., for the other). Across the hexagonal channel, ureas are parallel and are related by a twofold axis perpendicular to the channel. In the helical wheel diagrams, such ureas are given the same numerical indicator. In this manner, ureas 4 and 4' are related by a twofold axis, as are ureas 1 and 1', and so on. By convention, ureas in helix 1 lead with their C=O bond (represented as →) down the channel (away from the viewer), so in the diagram, ureas 1 and 1' are closest to the viewer, ureas 2 and 2' are 1.83 Å below 1 and 1', and so on. Because of

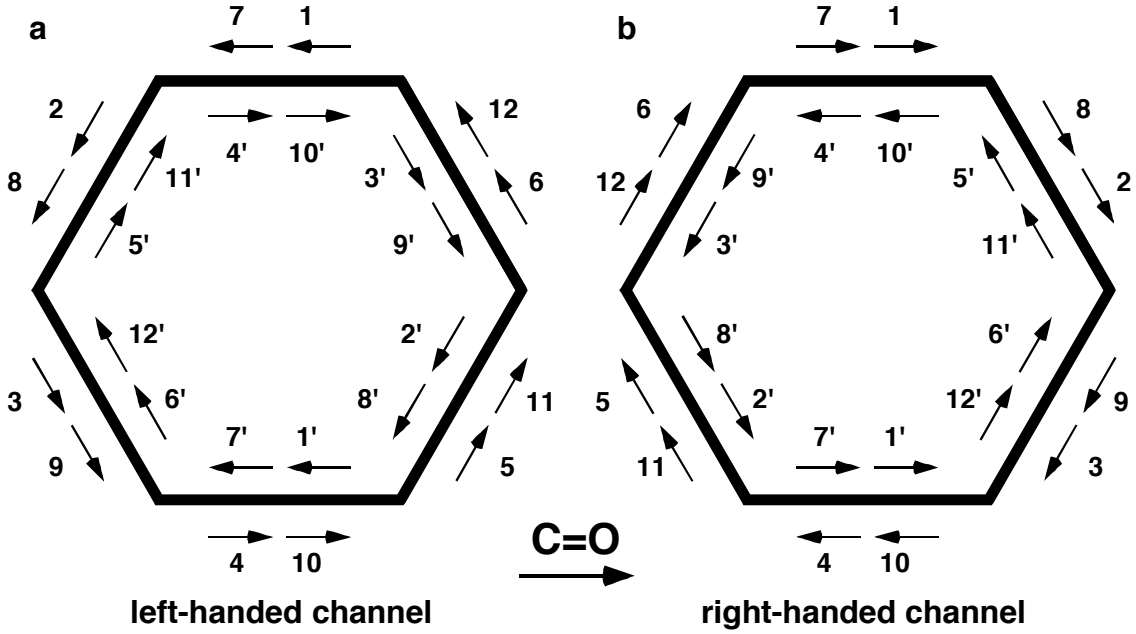


**Figure 1.7** Helical wheel diagrams for predicting host-guest hydrogen bonding patterns in UICs. Because the UIC channel is composed of a double helix, it is chiral and may be left-handed or right-handed. An example of each is depicted in **a** and **b**, respectively. The urea helices are related to one another by a twofold rotation about an axis perpendicular to the channel. Along the channel, ureas in helix 1 lead with their C=O axes (denoted by the arrows) as the channel winds into the page. Urea 1 is followed by urea 2, which is behind (below the plane of the page) of urea 1 by a distance of 1.84 Å. Following that is urea 3, then urea 4, etc. A complete turn of the helix comprises six urea molecules and spans a distance of (6 x 1.84 Å) = 11.0 Å. For the channel in **a**, the progression of these ureas along C=O bonds follows a left-handed spiral. For the channel in **b** this progression follows a right-handed spiral. Within each channel, members of the primed helix are labeled 1', 2', etc. By convention, ureas 1 and 1' are located at the same longitudinal position and have their C=O bonds, denoted by the arrows, oriented in the same direction. Because the pair of helices are related by twofold rotation, these ureas are related by the same twofold rotation, as are ureas 2 and 2', 3 and 3', etc. In the diagrams, the arrows for ureas 3 and 3' are pointed in the same direction; however, their progression along the channel is not the same. Within helix 1, ureas lead with their C=O; because the primed helix possesses the same handedness, its ureas lead in the opposite direction (with their *anti* N–H). Therefore, in the diagrams, ureas in helix 1 progress from 1, 2, 3, etc., in the direction of the arrows, while ureas in the primed helix progress from 1' to 2' to 3', etc., in the opposite fashion. Between helices, ureas in helix 1 hydrogen bond with ureas in helix 1' on adjacent channel walls. In this fashion, urea 4 forms a pair of $NH_{syn}$•••O hydrogen bonds with urea 2' as do ureas 12 and 10'. (In general, urea $n$+2 bonds with urea $n$'.) With an understanding of the stoichiometric relationship between host and guest, the helical wheels provide a simple means of predicting which ureas may form hydrogen bonds with the guest. The utility of this method is demonstrated in Figure 1.8. Helical wheels adapted from Brown, *et al.*, *Chemistry of Materials*, (1996), *8*, 1588.

their relative arrangements, ureas in the primed helix wind down the channel by leading with their *anti* N-H bonds (the tails of the arrows). In Figure 1.7a, each urea winds along its helix according to one's left hand; this channel is said to be left-handed. Analogously, Figure 1.7b presents a right-handed channel.

Diagrams such as these provide a simple means for predicting or rationalizing host-guest hydrogen bonding arrangements. Figure 1.8 presents the helical wheel diagrams for UICs of 2,10-undecanedione/urea and 2,9-decanedione/urea. These diagrams reflect the stereochemistry assumed in the respective crystal structures: a left-handed urea helix for 2,10-undecanedione/urea[71] and a right-handed urea helix[79] for 2,9-decanedione/urea. (For both crystals, the absolute stereochemistry is not known: these assignments were made arbitrarily because it was not possible to verify absolute stereochemistry using methods based upon anomalous dispersion.) For 2,10-undecanedione/urea, the commensurate relationship $2c_g' = 3c_h'$ provides a stoichiometry of one guest per nine host molecules. Because each donor urea forms hydrogen bonds with guests in two adjacent channels, this guest accepts hydrogen bonds from every tenth (inclusive) urea. Thus, there are four possible combinations of urea hydrogen bond donors: 1 and 10 (**a**), 1 and 10' (**b**), 1' and 10 (**c**), or 1' and 10' (**d**).

Immediately apparent in the diagrams of Figure 1.8 is the variation in guest torsions: for **b** and **c**, the guest O=C---C=O torsion angle is small, whereas for **a** and **d**, these carbonyls are pointed in opposite directions. At the outset, options **b** and **a** might appear to be enantiomers of options **c** and **d**, respectively. However, closer inspection reveals this is not the case. In **b**, the O=C---C=O torsion (from C2 to C10) runs clockwise (CW) along the channel as the left-handed helix winds counterclockwise

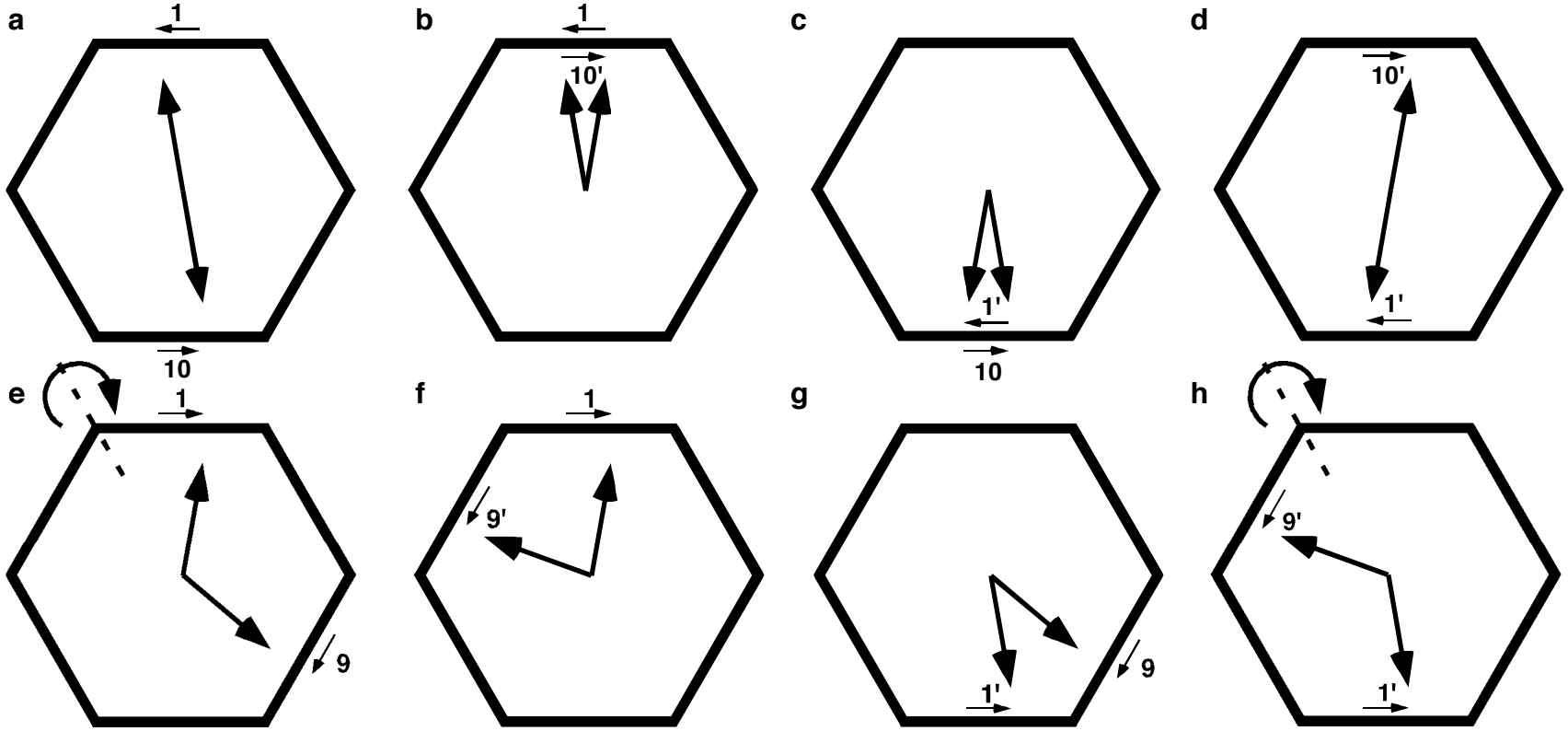


**Figure 1.8** Helical wheel diagrams for UICs of 2,10-undecanedione (left-handed helices, **a-d**) and 2,9-decanedione (right-handed helices, **e-h**). (**a-d**) For 2,10-undecanedione/urea, the commensurate relationship $2c_g' = 3c_h'$ provides a guest:host ratio of 1:9. Because each end of the guest is tethered to one-half of a urea molecule, 2,10-undecanedione hydrogen bonds with every tenth urea along the channel, which are separated by 16.5 Å. Thus, ureas 1 and 10' (**a**), 1 and 10 (**b**), 1' and 10 (**c**), or 1' and 10' (**d**) may donate a hydrogen bond to the guest depending on the torsion of the guest chain. Options **a** and **d** are related by a twofold rotation and are homomeric; options **b** and **c** exhibit enantiomeric guests in the same tunnel, making them diastereomeric. For this guest a torsion angle of ~0° between carbonyls is favored; the crystal structure in Figure 1.3 reflects option **b**. (**e-h**) For 2,9-decanedione/urea, the commensurate relationship $3c_g' = 4c_h'$ provides a guest:host ratio of 1:8. Depending on its torsion, 2,9-decanedione guest may form hydrogen bonds with ureas 1 and 9 (**e**), 1 and 9' (**f**), 1' and 9 (**g**), or 1' and 9' (**h**). Here, **e** and **h** are related by the twofold axis shown in **h**. For this guest, a torsion angle of ~180° between carbonyls is preferred, but is not compatible with a commensurate relationship between host and guest. A priori, options e (h) and f appear most promising. In the crystal structure, 2,9-decanedione guest coils so that the torsion angle between ketones is approximately 106° and the crystal structure described in Figure 1.5 reflects option **f.**

(CCW). For the guest in **c** this torsion is CCW for the same CCW helix. Because the helical sense of the urea channel is invariant, but the guest torsion is not, these options are diastereomeric. For **a** and **d**, simple twofold rotation about an axis running horizontal along the page demonstrates that these options are homomeric.

A simple consideration of 2,10-undecanedione (Figure 1.3a) suggests that this guest should favor a geometry in which the carbonyls are parallel (or nearly so). In this regard, options **a** and **d** appear to require unfavorable torsion of the guest chain and are therefore ruled out. In Figure 1.3, the crystal structure agrees with this prediction: the torsion angle between carbonyls is approximately 16°. For each end of the guest chain, hydrogen bonds should therefore be formed with ureas from different helices, as illustrated in models **b** and **c** of Figure 1.8. The torsion of the guest chain appears to counter the helical sense; thus, the guest winds CW as the left-handed host channel winds CCW. The actual structure matches the geometry predicted by option **b**.

Because it includes guests of presumably similar torsional energies, option **c** is a polymorph that may exist. However, in an investigation conducted by Dr. Matthew Peterson,[84] this polymorph was not observed even when different crystallization conditions were employed. To date, the small number of crystal structures that have been solved have all exhibited the type **b** structure, [59] whereas the diastereomeric polymorph depicted in Figure 1.8c has not been observed to date.

With 2,9-decanedione/urea (Figure 1.8e-h), the commensurate relationship $3c_g' = 4c_h'$ provides a stoichiometry of one guest per eight host molecules. As with 2,10-undecanedione/urea, each donor urea forms hydrogen bonds with guests in two channels (on either side of the channel wall); the guest:host stoichiometry ensures that each guest

accepts hydrogen bonds from every ninth (inclusive) urea. This allows four possible combinations of urea hydrogen bond donors: 1 and 9 (**e**), 1 and 9' (**f**), 1' and 9 (**g**), or 1' and 9' (**h**).

For this system, options **e** and **h** are rendered equivalent (homomeric) by a twofold rotation perpendicular to the channel axis (see arrow in Figure 1.8h). Structures **f** and **g**, on the other hand, are not related by symmetry. Instead, the hydrogen bond between host and guest is offset somewhat from the center of the channel wall so that carbonyls for the donor ureas may be directed towards one another (as in **g**) or away from one another (as in **f**). This means that guest O=C---C=O torsions in **f** and **g** differ; these options are therefore diastereomeric.

As discussed in Section 1.1.2, the extended conformation of 2,9-decanedione is slightly longer than necessary for the $3c_g' = 4c_h'$ repeat observed in the crystal structure of 2,9-decanedione/urea. Because the guest must coil up to fit, the ~180° O=C---C=O torsion angle present in the extended, all staggered conformation might not be expected. For options **e** and **h**, the guest carbonyls may assume torsion angles of approximately 120°; for **f** and **g**, the torsion angles are even smaller. In the crystal structure of 2,9-decanedione/urea, hydrogen bonding between the host and guest overcomes the unfavorable torsion energy of the guest: the O=C---C=O angle is approximately 106°, and the guests form hydrogen bonds with ureas 1 and 9'. These features are depicted in option **f**.

Helical wheel diagrams can, in many cases, be useful tools for understanding the possible torsional and hydrogen bond geometries for guests that hydrogen bond to the urea channel with both ends of their chain. Aside from the examples above, these

diagrams have been applied to several UIC systems, including 2,7-octanedione,[67] 2,12-tridecanedione,[81] and certain bis(acetate esters).[85] Helical wheel diagrams will be revisited in Chapter 5, where they are used to rationalize the possible guest positions of merohedral twins in ferroelastic UICs isostructural to 2,10-undecanedione/urea.

## 1.2 Shape Memory

One property closely related to ferroelasticity is shape memory.[33,34,86,87] Materials that exhibit the shape memory effect return to their initial (unstressed) form when heated to a particular temperature. This effect is related to *superelasticity*, which is a stress-induced martensitic phase transformation.[88,89] Both phenomena involve transformation from the austenite phase to the martensite phase. A special variety of shape memory, *rubber-like behavior* (RLB), was first discovered[35] in the 1930s for materials such as $Au_{52.5}Cd_{47.5}$. Strained samples of this alloy demonstrated elastic behavior (without heating) so that the author described them as being like rubber. Later workers have demonstrated RLB in a variety of alloys based on transition metals.[88] For these alloys, shape memory occurs in the martensitic state. Since both rubber-like behavior and superelasticity involve spontaneous recovery of strain (at constant temperature), they are examples of *pseudoelasticity.* Pseudoelasticity is characterized by the spontaneous recovery of strain (at constant temperature).[88] As discussed in the introduction section, martensitic phase transitions are characterized as involving lattice shears and other distortions of groups of atoms and do not include atomic (or molecular) diffusion, some of which are similar in nature to ferroelastic phase transitions.

Since its discovery, the origin of rubber-like behavior has been the subject of much debate.[90-93] The mechanism is now thought to involve mismatch between crystal defects and the domain that surrounds them;[94-96] this is illustrated in Figure 1.9, which is described below. Above some temperature, the material possesses high symmetry and is said to be in the austenite phase. Upon cooling to a phase of lower symmetry (martensite), the distribution of point defects (such as misplaced or vacant atoms) can adopt the symmetry of the macroscopic domain only over relatively long periods of time (ordinarily on the order of days). For freshly annealed samples in the martensitic phase, plastic behavior is observed because the defect distribution still retains the symmetry of the austenite and there is no driving force for shape memory. However, aged samples can exhibit rubber-like behavior. Although twins formed in a stressed crystal can potentially exhibit several domain orientations, the ones that best accommodate an applied stress will grow at the expense of others.[86,91] For the aged sample, the symmetry of the defect distribution has had time to adopt the symmetry of the unstressed phase so that it does not necessarily conform to the symmetry of the stress-induced twin. In this case, the *short-range order*, (SRO) of the point defects is said not to conform to the symmetry of the stress-induced twin.[96,97] This mismatch in symmetry destabilizes the crystal so that, once the stress has been removed, rubber-like behavior is observed.

Figure 1.9, adapted from the work of Ren and Otsuka[96], illustrates the proposed mechanism. In this model, the defect distribution of the austenite is constant throughout the crystal (Figure 1.9a). As this phase is cooled through the martensitic phase transition (Figure 1.9b), the annealed SRO is retained because the phase transition occurs on a much faster time scale than atomic diffusion. If the martensite in Figure 1.9b is stressed

immediately following this transition, defect ordering provides no energetic bias between states **b** and **c**, and plastic behavior is observed. However, if the martensite is aged, atomic diffusion can occur and the defect distribution adopts the macroscopic symmetry of the martensite. This "symmetry-conforming short-range ordering"[96] serves to stabilize state **d** with respect to **b** or **c** so that the martensitic phase transition temperature is increased for aged samples.[86] Furthermore, if **d** is stressed, the SRO does not conform to the daughter twin (Figure 1.9f) and destabilizes it. Stress release gives rise to the return of state **d** (rubber-like behavior).

If, however, the crystal is aged while under stress, the SRO of the crystal defects has time to conform to the symmetry of the stress-induced twin. This is illustrated in Figure 1.9g. Here, the SRO has adopted the symmetry of the daughter domain so that this twin is no longer destabilized with respect to **d**. Thus, the release of stress will not lead to pseudoelastic reversion because the deformed crystal is no longer destabilized by the SRO. Instead, the reconstituted SRO *stabilizes* this domain with respect to other potential twin orientations so that if the crystal is stressed once again, rubber-like behavior will result. The concept of point defect symmetry and its effect on domain stability has been extended to include the phase transition between austenite and martensite;[97] indeed, when briefly heated through the phase transition, the domain structure of the martensite can be preserved because the defect SRO has not yet adopted the symmetry of the high temperature phase. This is described by the transition between states in Figure 1.9d and e.

These properties are analogous to the ferroelastic behavior of UICs. For both systems, reversible domain reorientation accompanies the release of applied stress. Thus,

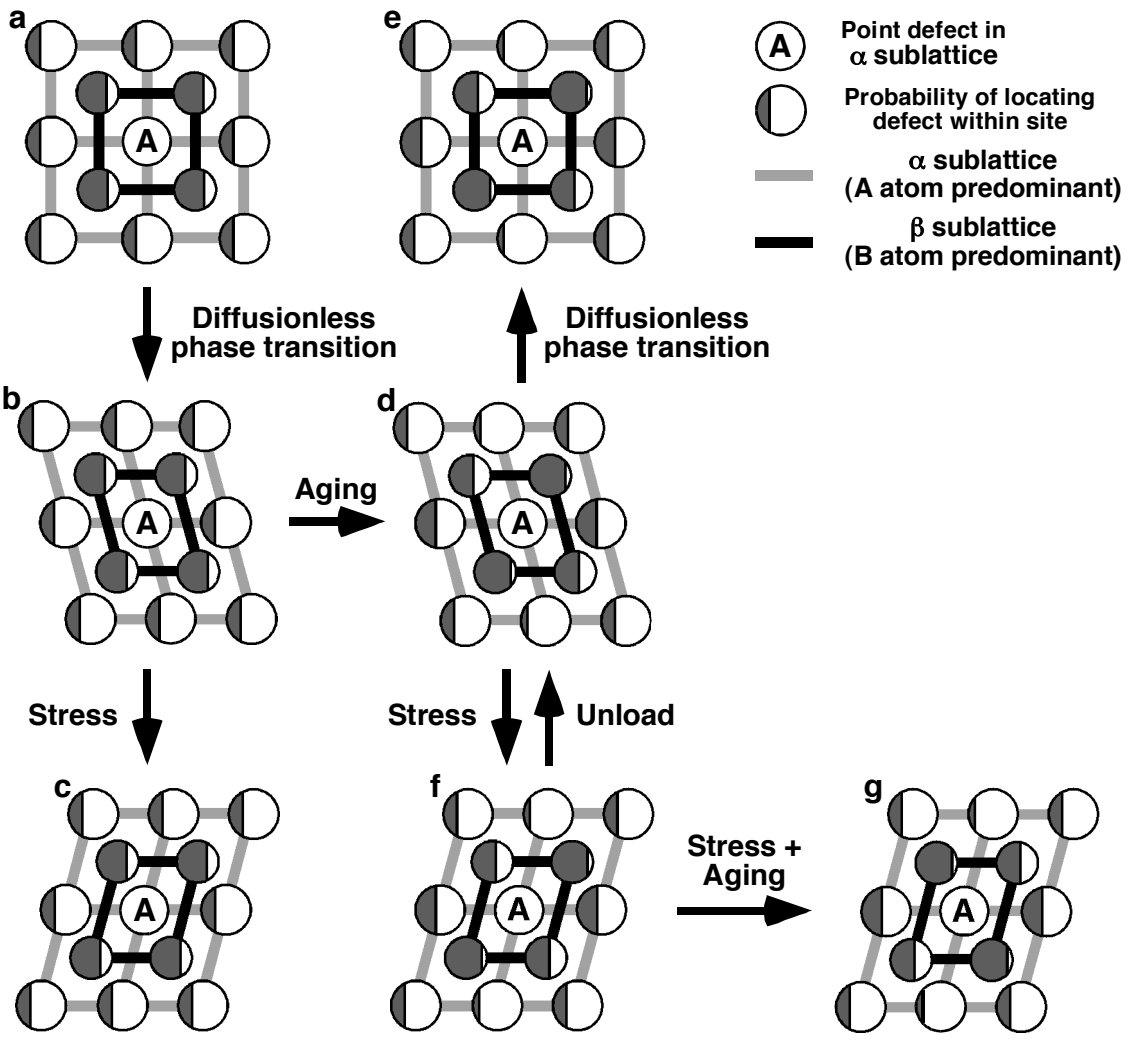


**Figure 1.9** The mechanism for rubber-like behavior in martensitic alloys, as proposed by Ren and Otsuka (see reference below). Here, the crystal lattice of an alloy containing α and β sublattices (see legend) is represented in two dimensions. For each lattice position neighboring site A the shading indicates the statistical probability of locating a point defect there. **(a)** The austenite phase. In this phase the probability for each site is the same. Upon cooling through the martensitic phase transition (to make **b**), these probabilities are preserved because the phase transition occurs on a shorter time scale than atomic diffusion. For martensite **b** the ordering of point defects around A inherited from austenite **a** does not conform to the symmetry of the martensite; this phase is therefore destabilized so that it exhibits plastic behavior if stressed immediately following the phase transition (**c**). **(d)** Upon aging, the distribution of defects surrounding A adopts the macroscopic symmetry of the martensite through atomic diffusion. Thus, the short range order, SRO, has conformed to the symmetry of the martensitic phase and the phase is no longer destabilized. If the aged martensite **d** is heated through the phase transition, the austenite **e** exhibits the same defect ordering until slow diffusion again equilibrates each site (to yield **a**). Because the SRO of **b** destabilizes this phase with respect to **d**, the martensitic transition temperature for **d** ⟶ **e** is greater than for **b** ⟶ **a**. If martensite **d** is stressed, the defect distribution destabilizes **f** so that rubber-like elasticity results. If martensite **f** is aged under stress, the defect distribution assumes a more stable SRO (as in **g**) and plastic behavior results. Figure drawn from Ren and Otsuka, *Nature (London)*, (1997), *389*, 579.

UICs and some shape memory alloys (two very different classes of solid material) have in common the property of pseudoelasticity. The work outlined in this thesis will serve to contrast the ferroelastic properties of martensitic alloys and UICs, as well as draw some important comparisons between their specific mechanisms.

## 1.3 The Plan

The purpose of this dissertation is to describe my accomplishments to this research program, while putting them into context with this research program and with the current understanding of ferroelastic materials and chemical crystallography. At the outset of these studies, some characteristics of UIC growth and ferroelasticity were misunderstood (or not fully appreciated). This work has helped to answer some of the many important questions, and has asked a few, as well. In describing these studies, there are two primary hypotheses that will be addressed:

### 1.3.1 Hypothesis I: UICs Grow According to Symmetry-Specific Mechanisms that Influence Lateral Guest Incorporation and/or Ordering

When viewed parallel to its long axis, the urea channel is hexagonal in shape, which corresponds to the hexagonal crystal morphologies of most UICs. Nominally, the point symmetry of the urea channel is hexagonal, but with guests such as 2,10-undecanedione the structure assumes an orthorhombic form. For any given crystal, the symmetry at the growth face is lower than the average crystallographic symmetry and will vary according to the exposed molecular functionality. Because crystal growth

occurs at the crystal surface, varying modes of guest incorporation are to be expected between growth faces with different structures.

This aspect of crystal growth has been exploited in the study of *solid solutions*, which are crystals that contain a mixture of chemical components. In their "general revision" of the formation of solid solutions, Lahav, Leiserowitz, and coworkers[98,99] and Bertman and McBride[100] demonstrated that the incorporation of impurities occurs in a nonrandom fashion. Constrained by symmetry, inequivalent growth sectors will exhibit preferential incorporation of different components, and these will be oriented in a polar manner.

For commensurate UICs incorporating bis(methyl ketones), solid solutions have been created by adding varying amounts of a *guest impurity*.[71,101] Typically, the impurities utilized are structurally very similar to the primary guest and can include monoketones, primary alkyl halides, esters, and *n*-alkanes. Growth models that rationalize the patterns of guest incorporation in UICs have been developed by Mark Hollingsworth;[102] these will be applied to the study of UICs such as 2,9-decanedione and 2,10-undecanedione. Using crystals containing two guests, preferential incorporation and ordering of guests will be demonstrated by observing changes in their optical behavior and by measuring differences in guest concentration using wet analytical methods.

### 1.3.2 Hypothesis II: Epitaxial Mismatch Between Domains Controls Memory Effects in Certain Ferroelastic UICs

Crystals of 2,10-undecanedione/urea are ferroelastic. For this material, domain switching involves the large-scale reorientation of crystalline regions that are associated

by a network of guest-host-guest hydrogen bonds that spreads throughout the crystal.[71] As illustrated in Figure 1.4, the daughter domain formed under stress does not retreat following the release of stress; this process is therefore irreversible, or *plastic*. Upon the introduction of a relaxive impurity,[101] 2-undecanone, spontaneously reversible domain switching, or rubber-like behavior, can be achieved.[71] Because it has only one hydrogen bond acceptor, this guest is tethered to the channel at only one end: its incorporation interrupts the interchannel host-guest network. In this way, relaxive impurities such as 2-undecanone lower the energetic barrier to domain switching so that spontaneous domain reversion may occur.

For a series of UICs containing mostly 2,10-undecanedione and some 2-undecanone, a correlation has been established between guest content and pseudoelastic reversion. In these studies, an abrupt change in reversion properties (a *critical threshold*) was observed. Using ultrafast videomicroscopy, the kinetics of domain reversion from daughter to mother in the fastest sites were shown not to depend appreciably on guest content. These studies, described in Chapter 4, help demonstrate how relaxive impurities can facilitate spontaneous reversion by speeding up the slow sites, whose domain wall motions are apparently inhibited in crystals containing smaller amounts of relaxive impurities.

Using synchrotron white-beam X-ray topography (SWBXT), Mark Hollingsworth and collaborators observed[103] nanoscopic domains in crystals of 2,10-undecanedione/urea. Because of their nanoscopic size, these domains are not observed in a typical stress experiment. Although they are epitaxially matched in the unstressed crystal, it is hypothesized that these domains become mismatched when bounded by

daughter. This mismatch is thought to provide a driving force for pseudoelastic reversion.[101] Spontaneous repair of mismatched defects, earlier observed in growing crystals of 2,10-undecanedione/urea, is hypothesized to be controlled by the same factors that drive domain reversion.[101] The mechanism by which nanoscopic domains affect ferroelastic behavior will be explored in Chapter 5 using optical and diffraction methods. This mechanism has several features in common with the mechanism of rubber-like behavior and may also be shared by other ferroelastics and shape-memory alloys.

These hypotheses and the studies undertaken to test them will be presented in the chapters that follow. Chapter 2 describes the study of symmetry and ordering in urea inclusion compounds. Chapter 3 discusses the low temperature phase transition in 2,9-decanedione/urea. Chapters 4 and 5 outline the current understanding of ferroelasticity in UICs containing 2,10-undecanedione and mixtures with 2-undecanone. Chapter 6 presents concluding remarks about the studies described. Finally, Chapter 7 outlines experimental methods, chemical syntheses and work not described in the main text.

## References Cited


1. Cahn, R. M. *The Coming of Materials Science*, (Pergamon, New York, 2001).
2. Schmidt, G. M. J. Photodimerization in the solid state. *Pure. Appl. Chem.* **27**, 647-678 (1971).
3. Cohen, M. D. & Schmidt, G. M. J. Topochemistry I. A survey. *J. Chem. Soc.*, 1996-2000 (1964).
4. Curtin, D. Y. & Paul, I. C. Chemical consequences of the polar axis in organic solid-state chemistry. *Chem. Rev.* **81**, 525-41 (1981).
5. Etter, M. C. Encoding and decoding hydrogen-bond patterns of organic compounds. *Acc. Chem. Res.* **23**, 120-6 (1990).
6. McBride, J. M., Segmuller, B. E., Hollingsworth, M. M. D. E. & Weber, B. A. Mechanical stress and reactivity in organic solids. *Science (Washington, D. C.)* **234**, 830 (1986).
7. McBride, J. M., Bertman, S. B. & Semple, T. C. Structural effects on surfaces within layered crystals. *Proc. Natl. Acad. Sci. USA* **84**, 4743-4746 (1987).
8. Holman, K. T., Pivovar, A. M., Swift, J. A. & Ward, M. D. Metric engineering of soft molecular host frameworks. *Acc. Chem. Res.* **34**, 107-118 (2001).
9. Aakeröy, C. B. & Salmon, D. J. Building co-crystals with molecular sense and supramolecular sensibility. *CrystEngComm* **7**, 439-448 (2005).
10. Hosseini, M. W. Molecular tectonics: From simple tectons to complex molecular networks. *Acc. Chem. Res.* **38**, 313-323 (2005).
11. Hollingsworth, M. D. Crystal engineering: From structure to function. *Science (Washington, D. C.)* **295**, 2410-2413 (2002).
12. Dunitz, J. D. & Gavezzotti, A. Molecular recognition in organic crystals: Directed intermolecular bonds or nonlocalized bonding? *Angew. Chem. Int. Ed.* **44**, 1766-1787 (2005).
13. Bernstein, J. *Polymorphism in Molecular Crystals*, (Oxford University Press, Oxford, 2002), p. 352.
14. Brunsteiner, M. & Price, S. L. Morphologies of Organic Crystals: Sensitivity of Attachment Energy Predictions to the Model Intermolecular Potential. *Cryst. Growth Des.* **1**, 447-453 (2001).
15. Motherwell, S. W., Ammon, H. L., Dunitz, J. D., Dzyabchenko, A., Erk, P., Gavezzotti, A., Hofmann, D. W., Leusen, F. J., Lommerse, J. P., Mooij, W. T., Price, S. L., Scheraga, H., Schweizer, B., Schmidt, M. U., van Eijck, B. P., Verwer, P. & Williams, D. E. Crystal structure prediction of small organic molecules: A second blind test. *Acta Crystallogr. B* **58**, 647 (2002).
16. Aizu, K. Possible species of "ferroelastic" crystals and of simultaneously ferroelectric and ferroelastic crystals. *J. Phys. Soc. Japan* **27**, 387-96 (1969).
17. Aizu, K. Possible species of ferromagnetic, ferroelectric, and ferroelastic crystals. *Phys. Rev. B* **2**, 754-772 (1970).
18. Wadhawan, V. K. *Introduction to Ferroic Materials*, (Gordon and Breach Science Publishers, Amsterdam, 2000), pp. 3-14.
19. Wadhawan, V. K. *Introduction to Ferroic Materials*, (Gordon and Breach Science Publishers, Amsterdam, 2000), pp. 14-28.

20. Mish, F. C., Editor in Chief. *"Ferro-", as defined in Webster's Ninth New Collegiate Dictionary*, (Merriam-Webster, Inc., Springfield, Massachusetts, 1988), p. 457.
21. Wadhawan, V. K. *Introduction to Ferroic Materials*, (Gordon and Breach Science Publishers, Amsterdam, 2000), pp. 14-15.
22. Wadhawan, V. K. *Introduction to Ferroic Materials*, (Gordon and Breach Science Publishers, Amsterdam, 2000), pp. 14-17 and 310-312.
23. Klapper, H. & Hahn, T. "Point-group symmetry and physical properties of crystals" in *International Tables for Crystallography, Volume A: Space-group symmetry. 5th (corrected) edition*, (ed. Hahn, T.) (Springer, Dordrecht, The Netherlands, 2005) pp. 804-808.
24. Aizu, K. Polarization, pyroelectricity, and ferroelectricity of ionic crystals. *Rev. Mod. Phys.* **34**, 550–576 (1962).
25. Lines, M. E. & Glass, A. M. *Principles and Applications of Ferroelectrics and Related Materials*, (Clarendon Press, Oxford, 1977), pp. 8-9.
26. Angel, R. J., Bismayer, U. & Marshall, W. G. Local and long-range order in ferroelastic lead phosphate at high pressure. *Acta Crystallogr. B* **60**, 1-9 (2003).
27. Lines, M. E. & Glass, A. M. *Principles and Applications of Ferroelectrics and Related Materials*, (Clarendon Press, Oxford, 1977), pp. 1-15.
28. Salje, E. Phase transitions in ferroelastic and co-elastic crystals. *Ferroelectrics* **104**, 111-20 (1990).
29. Roytburd, A. L. Principal concepts of martensitic theory. *J. Phys. IV* **5**, 21-30 (1995).
30. Wadhawan, V. K. *Introduction to Ferroic Materials*, (Gordon and Breach Science Publishers, Amsterdam, 2000), pp. 445-447.
31. Guymont, M. Symmetry analysis of structural phase transitions between phases not necessarily group-subgroup related. Domain structures. *Phys. Rev. B* **24**, 2647–2655 (1981).
32. Wadhawan, V. K. *Introduction to Ferroic Materials*, (Gordon and Breach Science Publishers, Amsterdam, 2000), pp. 123-124.
33. Otsuka, K. & Wayman, C. M. *Invitation to shape memory effect and the notion of martensitic transformation*, (Cambridge University Press, New York, 1998), pp. 2-5.
34. Kohl, M. *Shape Memory Microactuators*, (Springer, New York, 2004), pp. 25-36.
35. Ölander, A. An electrochemical investigation of solid cadmium-gold alloys. *J. Am. Chem. Soc.* **53**, 3819-3833 (1932).
36. Kurdyumov, G. & Khandros, L. G. *Dokl. Akad. Nauk. SSSR.* **66**, 211 (1949). Discussed by Cahn, R. M. Metallic rubber bounces back. *Nature (London)*, **374**, 120-121 (1995).
37. Lines, M. E. & Glass, A. M. *Principles and Applications of Ferroelectrics and Related Materials*, (Clarendon Press, Oxford, 1977), pp. 355-363.
38. Wöhler, F. On the artificial formation of urea. *Ann. Physik.* **12**, 253–256 (1828). Discussed by Cohen, P. S. and Cohen, S. M. Wöhler's synthesis of urea: How do the textbooks report it? *J. Chem. Ed.*, **73**, 883-886 (1996).

39. Cohen, P. S. & Cohen, S. M. Wöhler's synthesis of urea: How do the textbooks report it? *J. Chem. Ed.* **73**, 883-886 (1996).
40. Brewster, R. Q. *Organic Chemistry*, (Prentice-Hall, New York, 1948), pp. 2-3.
41. Dovesi, R., Causa, M., Orlando, R., Roetti, C. & Saunders, V. R. *Ab initio* approach to molecular crystals: A periodic Hartree-Fock study of crystalline urea. *J. Chem. Phys.* **92**, 7402-7411 (1990).
42. Rousseau, C., Van Alsenoy, C., Keuleers, R. & Desseyn, H. O. Solids modeled by *ab initio* crystal field methods. Part 17. Study of the structure and vibrational spectrum of urea in the gas phase and in its $P42_1m$ crystal phase. *J. Phys. Chem. A* **102**, 6540-6548 (1998).
43. Gao, D. & Williams, D. E. Molecular packing groups and *ab initio* crystal-structure prediction. *Acta Crystallogr. A* **55**, 621-627 (1999).
44. Sun, H. & Kung, P. W.-C. Urea: An *ab initio* and force field study of the gas and solid phases. *J. Comput. Chem.* **26**, 169-174 (2005).
45. Day, G. M., Price, S. L. & Leslie, M. Elastic constant calculations for molecular organic crystals. *Cryst. Growth Des.* **1**, 13-27 (2001).
46. Engkvist, O., Price, S. L. & Stone, A. J. Developments in computational studies of crystallization and morphology applied to urea. *Phys. Chem. Chem. Phys.* **2**, 3017-3027 (2000).
47. Halbout, J.-M. & Tang, C. L. "Properties and applications of urea" in *Nonlinear Optical Properties of Organic Crystals and Molecules*, vol. 1 (eds. Chemla, D. S. & Zyss, J.) (Academic Press, Inc., San Diego, 1987) pp. 385-404.
48. Bengen, F. & Schlenk, W., Jr. New addition products of urea. *Experientia* **5**, 200 (1949).
49. Swaminathan, S., Craven, B. M. & McMullan, R. K. The crystal structure and molecular thermal motion of urea at 12, 60 and 123 K from neutron diffraction. *Acta Crystallogr. B* **40**, 300-306 (1984).
50. George, A. R. & Harris, K. D. M. Representing and understanding geometric features of one-dimensional tunnel structures in solid inclusion compounds. *J. Mol. Graphics* **13**, 138-41 (1995).
51. Hollingsworth, M. D. & Harris, K. D. M. "Urea, Thiourea, and Selenourea" in *Comprehensive Supramolecular Chemistry*, vol. 6 (eds. MacNicol, D. D., Toda, F. & Bishop, R.) (Pergamon Press, New York, 1996) pp. 177-237.
52. Redlich, O., Gable, C. M., Dunlop, A. K. & Millar, R. W. Addition compounds of urea and organic substances. *J. Am. Chem. Soc.* **72**, 4153-4162 (1950).
53. Zimmerschied, W. J., Dinerstein, R. A., Weitkamp, A. W. & Marschner, R. F. Crystalline adducts of urea with linear aliphatic compounds. *Ind. Eng. Chem.* **42**, 1300-1306 (1950).
54. Harris, K. D. M. & Thomas, J. M. Structural aspects of urea inclusion compounds and their investigation by X-ray diffraction: A general discussion. *J. Chem. Soc., Faraday Trans.* **86**, 2985-96 (1990).
55. Le Gac, F., Toudic, B. & Hollingsworth, M. D. Unpublished observations; experiments conducted at the Université de Rennes (2005).

56. Lefort, R., Etrillard, J., Toudic, B., Guillaume, F., Breczewski, T. & Bourges, P. Incommensurate intermodulation of an organic intergrowth compound observed by neutron scattering. *Phys. Rev. Lett.* **77**, 4027-4030 (1996).
57. Lenné, H. U., Mez, H. C. & Schlenk, W., Jr. The lengths of molecules in inclusion channels of urea and thiourea. *Liebigs Ann. Chem.* **732**, 70-96 (1970).
58. Shannon, I. J., Harris, K. D. M., Rennie, A. J. O. & Webster, M. B. Theoretical prediction of the guest periodicity of alkane/urea inclusion compounds. *J. Chem. Soc., Faraday Trans.* **89**, 2023-9 (1993).
59. Hollingsworth, M. D. Personal communication to J. R. Rush (2007).
60. Harris, K. D. M. & Hollingsworth, M. D. Structural properties of the guest species in diacyl peroxide/urea inclusion compounds: An X-ray diffraction investigation. *Proc. Roy. Soc. A* **431**, 245-69 (1990).
61. Shannon, I. J., Stainton, N. M. & Harris, K. D. M. Structural properties of urea inclusion compounds containing carboxylic acid anhydride guest molecules: Anomalous modes of guest-molecule ordering. *J. Mater. Chem.* **3**, 1085-90 (1993).
62. Harris, K. D. M., Smart, S. P. & Hollingsworth, M. D. Structural properties of α,ω-dibromoalkane/urea inclusion compounds: A new type of interchannel guest molecule ordering. *J. Chem. Soc., Faraday Trans.* **87**, 3423-9 (1991).
63. Harris, K. D. M. Investigating the structure and dynamics of family of organic solids: The alkane/urea inclusion compounds. *J. Solid State Chem.* **106**, 83-98 (1993).
64. Fukao, K., Miyaji, H. & Asai, K. Anharmonic vibration of *n*-paraffin molecules in urea adducts. *J. Chem. Phys.* **84**, 6360-8 (1986).
65. Fukao, K. Disorder in paraffin chains of urea adducts and *n*-paraffins. *J. Chem. Phys.* **92**, 6867-74 (1990).
66. Shannon, I. J., Harris, K. D., Guillaume, F., Bocanegra, E. H. & MacLean, E. J. Phase transitions involving re-ordering of the guest molecules in a solid organic inclusion compound: Heptanoic anhydride–urea. *Chem. Commun.* **22**, 2341-2342 (1995).
67. Brown, M. E., Chaney, J. D., Santarsiero, B. D. & Hollingsworth, M. D. Superstructure topologies and host-guest interactions in commensurate inclusion compounds of urea with bis(methyl ketone)s. *Chem. Mater.* **8**, 1588-1591 (1996).
68. Hollingsworth, M. D., Peterson, M. L., Pate, K. L., Dinkelmeyer, B. D. & Brown, M. E. Unanticipated guest motion during a phase transition in a ferroelastic inclusion compound. *J. Am. Chem. Soc* **124**, 2094-2095 (2002).
69. Hollingsworth, M. D., Werner-Zwanziger, U., Brown, M. E., Chaney, J. D., Huffman, J. C., Harris, K. D. M. & Smart, S. P. Spring-loading at the molecular level. Relaxation of guest-induced strain in channel inclusion compounds. *J. Am. Chem. Soc.* **121**, 9732-9733 (1999).
70. Werner-Zwanziger, U., Brown, M. E., Chaney, J. D., Still, E. J. & Hollingsworth, M. D. Deuterium NMR studies of guest motions in urea inclusion compounds of 1,6-dibromohexane with analytical evaluation of spectra in the fast motion limit. *Appl. Magn. Reson.* **17**, 265-281 (1999).

71. Brown, M. E. & Hollingsworth, M. D. Stress-induced domain reorientation in urea inclusion compounds. *Nature (London)* **376**, 323-7 (1995).
72. Rush, J. R. Laboratory notebook entry jrr-f257. (2007).
73. Chatani, Y., Anraku, H. & Taki, Y. Phase transition and structure change of urea adducts with *n*-paraffins and paraffin-type compounds. *Mol. Cryst. Liq. Cryst.* **48**, 219-231 (1978).
74. Chatani, Y., Taki, Y. & Tadokoro, H. Low-temperature form of urea adducts with *n*-paraffins. *Acta Crystallogr. B* **33** (1977).
75. Smith, A. E. The crystal structure of the urea-hydrocarbon complexes. *Acta Crystallogr.* **5**, 224-235 (1952).
76. Forst, R., Jagodzinski, H., Boysen, H. & Frey, F. The disordered crystal structure of urea inclusion compounds $OC(NH_2)_2 + C_nH_{2n+2}$. *Acta Crystallogr. B* **46**, 70-78 (1990).
77. Forst, R., Boysen, H., Frey, F., Jagodzinski, H. & Zeyen, C. Phase transitions and ordering in urea inclusion compounds with *n*-paraffins. *J. Phys. Chem. Solids* **47**, 1089-97 (1986).
78. Hollingsworth, M. D. Laboratory notebook entry mdh-n-278-9. (2006).
79. Hollingsworth, M. D., Brown, M. E., Hillier, A. C., Santarsiero, B. D. & Chaney, J. D. Superstructure control in the crystal growth and ordering of urea inclusion compounds. *Science (Washington, D. C.)* **273**, 1355-1359 (1996).
80. Dewar, M. J. S., Zoebisch, E. G., Healy, E. F. & Stewart, J. J. P. Development and use of quantum mechanical molecular models. 76. AM1: A new general purpose quantum mechanical molecular model. *J. Am. Chem. Soc.* **107**, 3902-3909, (1985). Included in the Chem3D Pro software package, v. 3.5.1. CambridgeSoft Corporation (1997).
81. Hollingsworth, M. D., Brown, M. E., Dudley, M., Chung, H., Peterson, M. L. & Hillier, A. C. Template effects, asymmetry, and twinning in helical inclusion compounds. *Angew. Chem. Int. Ed.* **41**, 965-969 (2002).
82. Schlenk, W., Jr. Rotation of the plane of polarized light by hexagonal urea inclusion crystals. *Chem. Ber.* **101**, 2445-9 (1968).
83. Schlenk, W., Jr. Asymmetric urea inclusion lattice. IV. Absolute configuration of the lattice. *Liebigs Ann. Chem.* **7**, 1195-1209, (1973). This work was discussed by Hollingsworth, M. D. & Harris, K. D. M. "Urea, Thiourea, and Selenourea" in *Comprehensive Supramolecular Chemistry*, vol. 6 (eds. MacNicol, D. D., Toda, F. & Bishop, R.) (Pergamon Press, New York, 1996) pp. 177-237.
84. Peterson, M. L. Unpublished Observations (1999-2000).
85. Hollingsworth, M. D. Personal communication to J. R. Rush (2005).
86. Tadaki, T., Otsuka, K. & Shimizu, K. Shape-memory alloys. *Ann. Rev. Mater. Sci.* **18**, 25-45 (1988).
87. Wadhawan, V. K. *Introduction to Ferroic Materials*, (Gordon and Breach Science Publishers, Amsterdam, 2000), pp. 451-457.
88. Otsuka, K. & Wayman, C. M. *Mechanism of shape memory effect and superelasticity*, (Cambridge University Press, New York, 1998), pp. 27-48.
89. Wadhawan, V. K. *Introduction to Ferroic Materials*, (Gordon and Breach Science Publishers, Amsterdam, 2000), pp. 448-449.

90. Bhattacharya, K., James, R. D. & Swart, P. J. Relaxation in shape-memory alloys-part I. Mechanical mode. *Acta Mater.* **45**, 4547-4560 (1997).
91. Cahn, R. M. Metallic rubber bounces back. *Nature (London)* **374**, 120-121 (1995).
92. Zangwill, A. & Bruinsma, R. Origin of martensitic pseudoelasticity. *Phys. Rev. Lett.* **53**, 1073-6 (1984).
93. Lieberman, D. S., Schmerling, M. A. & Karz, R. W. "Ferroelastic "memory" and mechanical properties in gold-cadmium" in *Shape Memory Effects in Alloys*, (ed. Perkins, J.) (Plenum Press, Ltd., New York, 1975) pp. 203-244.
94. Suzuki, T., Tonokawa, T. & Ohba, T. Role of Short-Range Order in Martensitic Transformation. *J. Phys. IV* **5**, 1065-1070 (1995).
95. Marukawa, K. & Tsuchiya, K. Short-range ordering as the cause of the rubber-like behavior in alloy martensites. *Scripta Mater.* **32**, 77-82 (1995).
96. Ren, X. & Otsuka, K. Origin of rubber-like behaviour in metal alloys. *Nature (London)* **389**, 579-581 (1997).
97. Ren, X. & Otsuka, K. Universal symmetry property of point defects in crystals. *Phys. Rev. Lett.* **85**, 1016-1019 (2000).
98. Weissbuch, I., Popovitz-Biro, R., Lahav, M. & Leiserowitz, L. Understanding and control of nucleation, growth, habit, dissolution and structure of two- and three-dimensional crystals using 'tailor-made' auxiliaries. *Acta Crystallogr. B* **51**, 115-148 (1995).
99. Vaida, M., Shimon, L. J. W., Weisinger-Lewin, Y., Frolow, F., Lahav, M., Leiserowitz, L. & McMullan, R. K. The structure and symmetry of crystalline solid solutions: A general revision. *Science (Washington, D. C.)* **241**, 1475-1479 (1988).
100. McBride, J. M. & Bertman, S. B. Using crystal birefringence to study molecular recognition. *Angew. Chem. Int. Ed.* **28**, 330-333 (1989).
101. Hollingsworth, M. D., Peterson, M. L., Rush, J. R., Brown, M. E., Abel, M. J., Black, A. A., Dudley, M., Raghothamachar, B., Werner-Zwanziger, U., Still, E. J. & Vanecko, J. A. Memory and perfection in ferroelastic inclusion compounds. *Cryst. Growth Des.* **5**, 2100-2116 (2005).
102. Hollingsworth, M. D. Unpublished observations (2002).
103. Hollingsworth, M. D., Peterson, M. L., Dudley, M., Raghothamachar, B. & Dhanaraj, G. Unpublished observations. Experiments conducted at Brookhaven National Laboratory (2000).